NONLINEAR NONPERTURBATIVE OPTICS MODEL ENRICHED BY EVOLUTION EQUATION FOR POLARIZATION[*]

MARIANNA LYTOVA[†], EMMANUEL LORIN[†‡], AND ANDRÉ D. BANDRAUK[§‡]

Abstract. In this work, we extend and analyze the nonperturbative Maxwell-Schrödinger-Plasma (MASP) model. This model was proposed to describe the high order optical nonlinearities, and the low density free electron plasma generated by a laser pulse propagating in a gas. The MASP model is based on nonasymptotic, ab-initio equations, and accurately uses self-consistent description of micro (quantum)- and macro (field)- variables. However, its major drawback is a high computational cost, which in practice means that only short propagation lengths can be calculated. In order to reduce this cost, we study the MASP models enriched by a macroscopic evolution equation for polarization, from its simplest version in a form of transport equation, to more complex nonlinear variants. We show that homogeneous transport equation is a more universal tool to simulate the high harmonic spectra at shorter times and/or at a lower computational cost, while the nonlinear equation could be useful for modeling the pulse profiles when the ionization level is moderate. The gain associated with the considered modifications of the MASP model, being expressed in reduction of computational time and the number of processors involved, is of 2-3 orders of magnitude.

Key words. Maxwell-Schrödinger-Plasma equations, nonlinear optics, high harmonic generation, laser-filamentation

AMS subject classifications. 78A60, 78M20, 81V80

1. Introduction. The discovery of attosecond pulses [17, 34] and of laser filaments [12] has led to the need for an appropriate mathematical description of the evolution of ultrashort, that is only few-optical-cycles, laser pulses. Perturbative methods based on the approximate equations, e.g. Nonlinear Schrödinger Equation (NLSE)-type, although advantageous for not too short pulses, have essential intrinsic restrictions when applied to ultrashort pulses. These issues were addressed in some key papers [11, 19, 21]. Over the years, several advanced models were proposed, and we refer to a set of review papers [8, 16, 25]. Certain complex models, e.g. including High Order Kerr Effect (HOKE) and Unidirectional Pulse Propagation Equation (UPPE) [2, 24]), allow for accurate simulations and analysis of laser filamentation in some physical regimes [2, 7, 13, 26, 42, 48]. However, an appropriate modeling of free-electron plasma generated by the ultrashort intense laser pulse, as well as of nonperturbative evolution of the pulse in nonlinear media, is still an open problem that is only partially addressed [5, 6, 23, 35, 39, 40, 43, 45].

Now we briefly specify the principal features of the standard models used to study filament propagation [3, 8, 25]. In a broad sense, there are two general standard approaches to describe short-pulse propagation in a nonlinear medium [36, 38]:

- models considering the evolution of the envelope of the electromagnetic wave. As a rule, they are based on time-dependent NLSE, and the second generation equations, e.g. the Nonlinear Envelope Equation (NEE) [10];
- models based on full electric field propagators. It is the set of equations connected with Korteveg-de Vries (KdV) equation, e.g. the UPPE [38].

Applied to nonlinear optics, both "parental" equations, NLSE and KdV, as well as

[†]School of Mathematics and Statistics, Carleton University, Ottawa, Canada, K1S 5B6 (marianna.lytova@carleton.ca, elorin@math.carleton.ca).

[‡]Centre de Recherches Mathématiques, Université de Montréal, Montréal, Canada, H3T 1J4.

[§]Laboratoire de chimie théorique, Faculté des Sciences, Université de Sherbrooke, Sherbrooke, Canada, J1K 2R1 (andre.bandrauk@usherbrooke.ca).

their descendants, are reductions obtained under some assumptions from Maxwell's equations. To describe the linear and nonlinear response of the medium, the perturbative expansion for polarization vector with the susceptibility coefficients $\chi^{(2m+1)}$ was used [9]. In the strict sense, one can classify standard models as perturbative, even if they account HOKE [8].

Summing up, despite the quite reliable description of the evolution of the ultrafast laser pulses and relatively low computational cost, both standard approaches (i) use approximate but not exact propagation equations; (ii) employ perturbative expansion for the polarization; (iii) receive the frequency-property of the medium as an external parameters; (iv) compute free electron density phenomenologically [8, 25]. All these properties suggest that the solution of the problem can be improved and the involvement of non-standard nonperturbative models will be highly useful. The fully self-consistent mathematical model must include side by side [27, 29]:

- Maxwell's equations (MEs) modeling the evolution of the laser field under the response of the molecules in the gas region where the pulse propagates;
- the set of time-dependent Schrödinger equations (TDSEs), which describes the interaction of the molecules with an electromagnetic field of the pulse;
- kinetic equations, in order to take into account the dynamics of the generated free-electron plasma.

In practice, the realization of such Maxwell-Schrödinger-Plasma (MASP) model [27] faces extremely high computational cost for solving the system of TDSEs, and requires high performance computing. Nevertheless, over the past 10 years important results have been achieved within this model, and the studies are in progress, see e.g. [27, 28, 29, 31, 32]. Namely, it was suggested [30, 31] to enrich the MASP model by a *macroscopic* transport equation modeling the nonperturbative polarization. It was demonstrated that this approach allows to reduce drastically the number of *microscopic* TDSEs in the model thus making the numerical computation of the model much faster. The goals of this paper is (i) to justify mathematically well-posedness of the thus supplemented MASP model, and (ii) to derive more accurate and sophisticated evolution equations.

This paper is organized as follows. In Section 2, we derive the MASP equations enriched by the evolution equations modeling the propagation of the polarization. Section 3 is devoted to the mathematical analysis of the enriched model. Numerical approximation and parallel computing aspects are addressed in Section 4. Several numerical experiments are presented in Section 5. We finally conclude in Section 6.

2. MASP Model and its Development. The usual spatial setting is as follows: the electromagnetic pulse propagates in sequence through 3 regions: vacuum, molecule-gas and again vacuum. As soon as the wave envelope gets into the last vacuum region, the electric field components in space and time are stored. The starting point is a *micro-macro* model constituted by MEs coupled with several TDSEs, describing the nonlinear response of gas subject to an electromagnetic field [27, 28, 29]. More precisely, to simulate the *macroscopic* propagation effects, we use the differential form of Ampere-Maxwell's and Faraday-Maxwell's laws in a bounded spatial domain Ω, with a smooth boundary $\partial\Omega$. We define $\mathbf{x}' = (x', y', z')^T$ the electromagnetic field space variable, then for nonmagnetic medium, $\mathbf{B} = \mathbf{H}$:

(1a) $$\partial_t \mathbf{E}(\mathbf{x}', t) = c\nabla \times \mathbf{B}(\mathbf{x}', t) - 4\pi(\partial_t \mathbf{P}(\mathbf{x}', t) + \mathbf{J}(\mathbf{x}', t)),$$

(1b) $$\partial_t \mathbf{B}(\mathbf{x}', t) = -c\nabla \times \mathbf{E}(\mathbf{x}', t).$$

Thus, to compute from (1a) and (1b) the electromagnetic field vectors $\mathbf{E}(\mathbf{x}',t)$ and $\mathbf{B}(\mathbf{x}',t)$, we need to determine the polarization $\mathbf{P}(\mathbf{x}',t)$ and the current density $\mathbf{J}(\mathbf{x}',t)$ vectors from the microscopic equations.

We will consider interaction between a molecule, typically H_2^+ for simplicity, and the field in the dipole approximation, which is valid when the smallest internal wavelengths $\lambda_{\min}$ of the electromagnetic field are much larger than the molecule size ℓ (in the same direction), that is $\ell \ll \lambda_{\min}$. Typically we have $\lambda_{\min} \approx 800$ nm (Ti:Sapphire laser) and for H_2^+-molecule size $\ell \approx 0.1$ nm. The simple molecule H_2^+ possesses two advantages: it has only one electron, and is symmetric with respect to the point bisecting the interval between the nucleus. It follows the symmetry of the Hamiltonian with respect to the electron coordinate inversion: $\mathbf{x} \longrightarrow -\mathbf{x}$, which allows to reduce formally the problem of describing the dynamics of 3 particles, to a 2-body problem, and hence the exact Schrödinger equation can be numerically considered [28]. However, in practice, even more complex molecules like O_2, N_2 could as well be considered within the MASP, using the single active electron approximation (SAE), [41].

Although in its whole generality the MASP model for H_2^+ includes the motion of the 3 particles [28], we will use the Born-Oppenheimer approximation throughout the article. It is a typical approximation in quantum chemistry, since the time-scale for dynamics of the interatomic electrons (attoseconds) is much shorter then the time-scale for the nuclei motion (femtoseconds) [14, 37, 50]. At the molecular (*microscopic*) scale, we will denote by $\mathbf{x} = (x, y, z)^T$ the TDSEs space variable (that is for electron wavefunctions). The components of the polarization vector $\mathbf{P}(\mathbf{x}',t)$, be to substituted into MEs (1a) and (1b), are computed using a trace operator [27]:

$$(2a) \quad \mathbf{P}(\mathbf{x}',t) = \mathcal{N}(\mathbf{x}') \sum_{i=1}^{m} \mathbf{P}_i(\mathbf{x}',t) = -\mathcal{N}(\mathbf{x}') \sum_{i=1}^{m} \chi_{\Omega_i}(\mathbf{x}') \int_{\mathbb{R}^3} \psi_i^*(\mathbf{x},t) \mathbf{x} \psi_i(\mathbf{x},t) d\mathbf{x},$$

$$(2b) \quad i\partial_t \psi_i(\mathbf{x},t) = -\frac{\Delta_{\mathbf{x}}}{2} \psi_i(\mathbf{x},t) + V_C(\mathbf{x})\psi_i(\mathbf{x},t) + \mathbf{x} \cdot \mathbf{E}_{\mathbf{x}_i'}(t)\psi_i(\mathbf{x},t), \ \forall i \in \{1,..,m\},$$

where V_C denotes the *static* interaction potential. The density of ionic molecule H_2^+ is taken to be smooth in space, and is denoted by $\mathcal{N}(\mathbf{x}')$. It must be approximately equal to the initial electrons number density $\mathcal{N}_{e0}(\mathbf{x}')$ [15], and can be assumed constant in time in case of low level of ionization. For example, let the ionic H_2^+-molecule be oriented in the plane (x,y) of the selected Cartesian system, then the nuclear potential is written as:

$$(3) \quad \begin{aligned} V_C(\mathbf{x}) = &-\left[\left(x - \frac{R_0}{2}\cos\theta\right)^2 + \left(y - \frac{R_0}{2}\sin\theta\right)^2 + z^2\right]^{-1/2} - \\ &-\left[\left(x + \frac{R_0}{2}\cos\theta\right)^2 + \left(y + \frac{R_0}{2}\sin\theta\right)^2 + z^2\right]^{-1/2}, \end{aligned}$$

where $\theta \in [0°, 90°]$ defines the angle between the molecular axis of H_2^+ and the x-axis, with an internuclear distance R_0; in our computations it usually equals to 2 atomic units (a.u.), corresponding to ≈ 0.1 nm, see e.g. [50].

Solving of the TDSEs (2b) provides a complete set of the wavefunctions, which in its turn allows to evaluate the ionization level of a gas and obtain a continuum spectrum of free electrons propagating in a laser pulse. We define the spatial domain $\Omega = \cup_{i=1}^m \Omega_i$, where Ω_i denotes the *macroscopic* spatial domain containing a molecule of reference associated to a wavefunction ψ_i, while in (2a) $\mathbf{P}_i(t) = \chi_{\Omega_i}\mathbf{d}_i(t)$ denotes the *macroscopic* polarization in this domain, and the index i is associated to the specific coordinate of MEs, $\mathbf{x}'$. Functions χ_{Ω_i} are defined as $\chi \otimes \mathbf{1}_{\Omega_i}$ where χ is

a plateau, and $\mathbf{1}_{\Omega_i}$ is the characteristic function of Ω_i. Also $\mathbf{d}_i(t)$ is a *microscopic* time-dependent dipole moment of a molecule belonging to Ω_i:

$$(4) \qquad \mathbf{d}_i(t) = -\int_{\mathbb{R}^3} \psi_i^*(\mathbf{x},t)\mathbf{x}\psi_i(\mathbf{x},t)d^3\mathbf{x}.$$

In other words, the domain Ω_i contains $\mathcal{N}(\mathbf{x}')\mathrm{vol}(\Omega_i)$ molecules represented by one single wavefunction ψ_i (under the assumption of a unique pure state [27]). We now assume that the spatial support of ψ_i is included in a domain $\omega_i \subset \mathbb{R}^3$. We allow free electrons to reach the boundary $\partial\omega_i$, where we impose artificial complex potential, see e.g. [18]. Thus, in the discussed model, the part of the wavefunction absorbed at the boundary generates the plasma of free electrons. Finally in (2b), $\mathbf{E}_{\mathbf{x}_i'}$ denotes the electric field (supposed to be constant within ω_i) in Ω_i.

To close the set of equations, the current density evolution equation can be integrated in the system via the Drude model [8, 28] on the MEs domain:

$$(5) \qquad \partial_t \mathbf{J}(\mathbf{x}',t) + \nu_e \mathbf{J}(\mathbf{x}',t) = \mathcal{N}_e(\mathbf{x}',t)\mathbf{E}(\mathbf{x}',t),$$

where ν_e denotes the effective electron collision frequency. In the MASP model $\mathcal{N}_e(\mathbf{x}',t)$ is computed from molecular ionization self-consistently:

$$(6) \qquad \mathcal{N}_e(\mathbf{x}',t) = \mathcal{N}_{e0}(\mathbf{x}') + \mathcal{N}(\mathbf{x}')\sum_{i=1}^{m} \chi_{\Omega_i}(\mathbf{x}')\mathcal{I}_i(t),$$

where the function

$$(7) \qquad \mathcal{I}_i(t) = 1 - \int_{\Omega_i} |\psi_i(\mathbf{x},t)|^2 d^3\mathbf{x}$$

defines a fraction of the electrons freed due to tunnel ionization [22, 1], using the L^2-norm of the bound electron wavefunctions.

Remark 2.1. Equations (1a), (1b), (2a), (2b), and (5) form the MASP model.

In general, for 1-electron TDSE and under Born-Oppenheimer approximation, the MASP model is 3d-3d in the sense, that $\mathbf{E}(\mathbf{x}',t)$, $\mathbf{B}(\mathbf{x}',t)$ and $\psi(\mathbf{x},t)$ are functions of spatial coordinates: $\mathbf{x}' = (x',y',z')^T$ and $\mathbf{x} = (x,y,z)^T$. More generally, in the terminology Md-Nd, $M = \dim(\mathbf{x}')$ and $N = \dim(\mathbf{x})$. In practice, we can reduce the computational complexity of the system by applying a reasonable dimensionality reduction. For example, Figure 1 illustrates domain decomposition in case of 1d-2d MASP model with the pulse propagating in the z'-direction.

However, if we want to describe the medium response to a laser pulse within the MASP model accurately, a very large number of TDSEs is required, increasing immensely the overall computational cost of the model. With the purpose to reduce this cost, Lorin et al. [30, 31] have proposed to enrich the MASP model by a simple transport equation for polarization:

$$(8) \qquad \partial_t \mathbf{P}(\mathbf{x}',t) + v_g \partial_{z'}\mathbf{P}(\mathbf{x}',t) = \mathbf{0},$$

where v_g is the group velocity. More specifically, the MEs domain is now decomposed along the z'-direction in N_1 subdomains, each containing N_2 *layers* transversal to z'-axis with thickness $\Delta z'$. For the 3d MEs, the dimensionality of such a layer is 2: plane (x',y'), while in case of 1d MEs the "layer" degenerates to the cell,
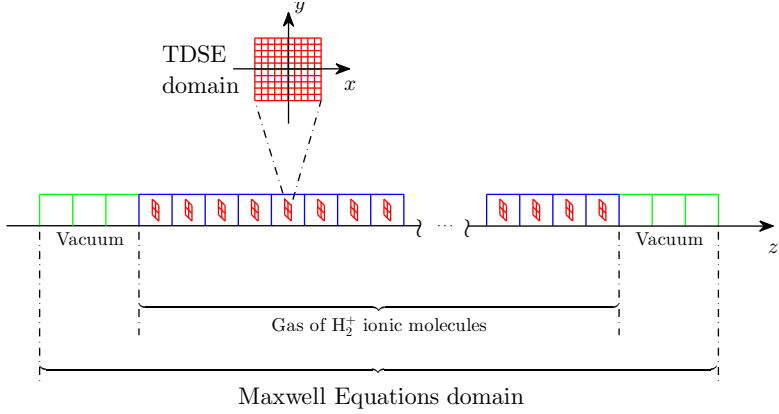
FIG. 1. *Spatial domain decomposition for the 1d-2d (macro-micro) spatially approximated MASP model.*

whose transversal dimension is 0. In order to locally evaluate the dipole moment, the TDSEs are computed only at first layers (or cells) of each subdomain with coordinates denoted $\mathbf{x}'_{\alpha,1}$, where $\alpha = 1, \ldots, N_1$, and the second index is for the number of layer/cell within the subdomain. Thus, we can add to (8) the initial value of polarization $\mathbf{P}(\mathbf{x}'_{\alpha,1}, 0) = \mathcal{N}(\mathbf{x}'_{\alpha,1})\mathbf{d}(\mathbf{x}'_{\alpha,1}, 0)$. Between these first layers/cells, the evolution equations on $\mathbf{P}$, such as (8), are used for a "cheap" computation (as fully macroscopic) of the polarization vector. For the 1d-2d MASP model this methodology is summarized in Figure 2.

Note that this model is applicable as long as the length $\Delta_\alpha z'$ of the subdomains along z'-axis is short enough, or/and if the molecule density is low enough. That is, as long as the effect of the medium on $\mathbf{E}$ during the pulse propagation from $\mathbf{x}'_{\alpha,1}$ to $\mathbf{x}'_{\alpha+1,1}$ is sufficiently negligible not to be included in the dipole moment calculation of a molecule located at $\mathbf{x}'_{\alpha+1,1}$. In order to include the medium effects on $\mathbf{E}$ during the propagation in $(\mathbf{x}'_{\alpha,1}, \mathbf{x}'_{\alpha+1,1})$, an improvement of the model is necessary.

The approach we propose here allows to consider larger propagation lengths and times more accurately than the simple transport equation. Since we consider multidimensional EM field propagation, including forward and backward propagation effects,
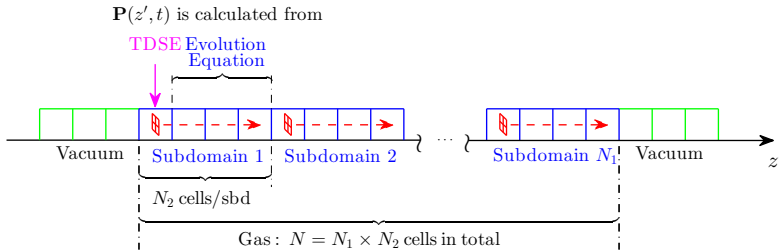
FIG. 2. *Spatial domain decomposition for the 1d-2d MASP model enriched by the evolution equation for polarization.*

the equation for polarization is expected to be of the form:

$$(9) \qquad \partial_t^2 \mathbf{P} - v_g^2 \triangle \mathbf{P} = \mathbf{S}(\mathbf{E}),$$

where for brevity sake we denote $\mathbf{P} \equiv \mathbf{P}(\mathbf{x}', t)$, $\mathbf{E} \equiv \mathbf{E}(\mathbf{x}', t)$. The main idea consists of including as much information as possible to determine $\mathbf{S}(\mathbf{E})$ in (9). Cancelling out $\mathbf{B}$ from (1a) and (1b), we get the wave equation for $\mathbf{E}$:

$$(10) \qquad \partial_t^2 \mathbf{E} - c^2 \triangle \mathbf{E} + c^2 \nabla(\nabla \cdot \mathbf{E}) = -4\pi(\partial_t^2 \mathbf{P} + \partial_t \mathbf{J}).$$

We omit the term $\nabla(\nabla \cdot \mathbf{E})$, supposing that on the relevant propagation length non-linearity is not very strong, as $\nabla \cdot \mathbf{E} \propto \nabla \cdot \mathbf{P}^{NL}$ [9]:

$$(11) \qquad \partial_t^2 \mathbf{E} - c^2 \triangle \mathbf{E} = -4\pi(\partial_t^2 \mathbf{P} + \partial_t \mathbf{J}).$$

Next, we assume that the perturbative expansion

$$(12) \qquad \mathbf{P}(\mathbf{x}', t) = \chi^{(1)} \mathbf{E}(\mathbf{x}', t) + \chi^{(3)} (\mathbf{E}(\mathbf{x}', t) \cdot \mathbf{E}(\mathbf{x}', t)) \mathbf{E}(\mathbf{x}', t),$$

where $\chi^{(1)}$ and $\chi^{(3)}$ are the first and third *instantaneous* susceptibilities of isotropic medium is an accurate approximation for $\mathbf{P}$ at least *for short enough propagation length*. From here

$$(13) \qquad \mathbf{E}(\mathbf{x}', t) = \frac{1}{\chi^{(1)}} \mathbf{P}(\mathbf{x}', t) - \frac{\chi^{(3)}}{\chi^{(1)}} (\mathbf{E}(\mathbf{x}', t) \cdot \mathbf{E}(\mathbf{x}', t)) \mathbf{E}(\mathbf{x}', t).$$

Then substituting (13) in (11) leads to

$$(14) \quad (1 + 4\pi\chi^{(1)})\partial_t^2 \mathbf{P} - c^2 \triangle \mathbf{P} = \chi^{(3)} \Big[\partial_t^2 \big(\mathbf{E}(\mathbf{E} \cdot \mathbf{E}) \big) - c^2 \triangle \big(\mathbf{E}(\mathbf{E} \cdot \mathbf{E}) \big) \Big] - 4\pi\chi^{(1)} \partial_t \mathbf{J},$$

where $(\mathbf{E} \cdot \mathbf{E}) = E_x^2 + E_y^2 + E_z^2$. The group velocity in the first approximation can be defined as $v_g = c/\sqrt{1 + 4\pi\chi^{(1)}}$ [31], so that the evolution equation for $\mathbf{P}$ is shaped into

$$(15) \qquad \partial_t^2 \mathbf{P} - v_g^2 \triangle \mathbf{P} = \left(\frac{v_g}{c}\right)^2 \Big\{ \chi^{(3)} \Big[\partial_t^2 (\mathbf{E}\mathbf{E}^2) - c^2 \triangle (\mathbf{E}\mathbf{E}^2) \Big] - 4\pi\chi^{(1)} \partial_t \mathbf{J} \Big\}.$$

At preselected locations, say $\mathbf{x}'_\alpha$ ($\alpha = 1, 2 \ldots N_1$) and at each computational time step t_β, the data $\mathbf{P}(\mathbf{x}'_\alpha, t_\beta)$, $\partial_t \mathbf{P}(\mathbf{x}'_\alpha, t_\beta)$ are computed from microscopic TDSEs:

$$(16) \qquad \begin{cases} \mathbf{P}(\mathbf{x}'_\alpha, t_\beta) = \mathcal{N}(\mathbf{x}'_\alpha) \int_{\mathbb{R}^3} \big| \psi_{\mathbf{x}'_\alpha}(\mathbf{x}, t_\beta) \big|^2 \mathbf{x} d^3\mathbf{x}, \\ \partial_t \mathbf{P}(\mathbf{x}'_\alpha, t_\beta) = \mathcal{N}(\mathbf{x}'_\alpha) \int_{\mathbb{R}^3} \partial_t \big| \psi_{\mathbf{x}'_\alpha}(\mathbf{x}, t_\beta) \big|^2 \mathbf{x} d^3\mathbf{x}. \end{cases}$$

Recall that the current density $\mathbf{J}$ satisfies the macroscopic kinetic equation (5). Let the free electron density be a function of the z'-coordinate, the direction of the pulse propagation, and time. It is reasonable then to compute this value from the following transport equation:

$$(17) \qquad \partial_t \mathcal{N}_e(z', t) + v_g \partial_{z'} \mathcal{N}_e(z', t) = 0,$$

with the initial distribution computed according to (6) and (7):

$$(18) \qquad \mathcal{N}_e(z'_\alpha, t_\beta) = \mathcal{N}_{e0}(z'_\alpha) + \mathcal{N}(z'_\alpha) \sum_{i=1}^{m} \chi_{\Omega_i}(z'_\alpha) \Big[1 - \int_{\Omega_i} |\psi_i(\mathbf{x}, t_\beta)|^2 d^3\mathbf{x} \Big].$$

Thus, except for the evaluation of the polarization and the free electron number density at specific locations, requiring TDSE computations, the evolution equations (15) and (17) are then fully macroscopic.

Remark 2.2. Equations (1a), (1b), and (5) defined on a bounded spatial domain Ω, being coupled to the evolution equations for polarization (15) (or in the simplest case, to equation (8)) and to the evolution equations for free electron density (17) with respective initial conditions (16) and (18), computed at the set of preselected locations of Ω through the TDSEs (2b), form the enriched MASP model.

It is necessary to comment the philosophy of the proposed approach. Equations (15) with initial conditions (16) form a nonperturbative model, which includes (i) the transport of *nonperturbative* data (as $\partial_t \mathbf{P}_0$ are computed from TDSEs) from the left boundary to the right one of each subdomain, and (ii) the *perturbative* corrections to polarization within these subdomains. In (8), we do not assume propagation in a linear medium, however, we use a linear approximation that is valid when the length of the subdomain is short enough, and the same was assumed while deriving (15) from (11) and (12). Thus, in our *model approach* the LHS in the equation (15) represents the linear transport of the *nonperturbative* polarization $\partial_t \mathbf{P}(\mathbf{x}'_\alpha, \cdot)$ initially taken from the nonperturbative computations (16) at reference points $\mathbf{x}'_\alpha$, $\alpha = 1, \ldots, N_1$, across the subdomains. The RHS of the equation (15) makes the non-zero *perturbative* corrections to the polarization in interval $\Delta_\alpha z'$.

For practical purposes, we simplify the polarization evolution equation in the case of 1d-2d model, moreover we will consider the case of linearly polarized pulse, implying that $P_{x'}(z', t)$ as well as $E_{x'}(z', t)$ are null. Thus, assuming that the polarization vector propagates along the z'-direction (Laplacian $\triangle$ is reduced to $\partial_{z'}^2$) we obtain an evolution equation for $P_{y'}$:

$$(19) \quad \begin{aligned} \partial_t^2 P_{y'} - v_g^2 \partial_{z'}^2 P_{y'} &= 3\chi^{(3)} \left(\frac{v_g}{c}\right)^2 E_{y'}^2 \left[\partial_t^2 E_{y'} - c^2 \partial_z^2 E_{y'}\right] + \\ &\quad + 6\chi^{(3)} \left(\frac{v_g}{c}\right)^2 E_{y'} \left[(\partial_t E_{y'})^2 - c^2 (\partial_{z'} E_{y'})^2\right] - 4\pi\chi^{(1)} \left(\frac{v_g}{c}\right)^2 \partial_t J_{y'}. \end{aligned}$$

For the sake of simplicity of the notation we introduce three variable factors

$$(20) \quad \begin{aligned} a(E_{y'}(z', t)) &:= 1 + 12\pi\chi^{(3)}(v_g/c)^2 E_{y'}^2, \\ b(E_{y'}(z', t)) &:= 6\chi^{(3)}(v_g/c)^2 E_{y'}, \\ g(E_{y'}(z', t)) &:= 4\pi(v_g/c)^2(\chi^{(1)} + 3\chi^{(3)} E_{y'}^2), \end{aligned}$$

and observing that $\partial_t^2 E_{y'} - c^2 \partial_{z'}^2 E_{y'} = -4\pi\partial_t^2 P_{y'} - 4\pi\partial_t J_{y'}$ in 1d, the polarization wave equation takes the form

$$(21) \quad \begin{aligned} a(E_{y'})\partial_t^2 P_{y'} - v_g^2 \partial_{z'} P_{y'} &= \\ &= b(E_{y'})\left[(\partial_t E_{y'})^2 - c^2(\partial_z E_{y'})^2\right] - g(E_{y'})\partial_t J_{y'}. \end{aligned}$$

Recall that we want to couple this equation to the MASP model. However, the RHS of (21) contains partial derivatives of the electric field in time, and this fact may result in some sort of computational instability. To avoid possible instability of the solution, we replace in (21) $\partial_t E_{y'} = c\partial_{z'} B_{x'} - 4\pi\partial_t P_{y'} - 4\pi J_{y'}$ according to (1a), thus

$$(22)$$
$$\begin{aligned} a(E_{y'})\partial_t^2 P_{y'} - v_g^2 \partial_{z'}^2 P_{y'} + 8\pi b(E_{y'})\left[(c\partial_z B_{x'} - 4\pi J_{y'})(\partial_t P_{y'}) - 2\pi(\partial_t P_{y'})^2\right] &= \\ = b(E_{y'})\left\{c^2\left[(\partial_{z'} B_{x'})^2 - (\partial_z E_{y'})^2\right] + 8\pi J_{y'}\left[2\pi J_{y'} - c\partial_{z'} B_{x'}\right]\right\} - g(E_{y'})\partial_t J_{y'}. \end{aligned}$$

Finally, we provide the principal details of the procedure leading to the 1d-2d enriched MASP model.

- At $t = t_\beta$, all the time derivatives of polarization $\partial_t P_{y'}(z'_{\alpha,1}, t_\beta)$ are computed at locations with coordinates $z'_{\alpha,1}$, $\alpha = 1, \dots N_1$, from the set of TDSEs (2b) according to (16), see Figure 2;
- These data are used as boundary conditions for the wave equation (22) with $\partial_{z'} B_{x'}(z', t_\beta)$ and $\partial_{z'} E_{y'}(z', t_\beta)$ in the RHS, in order to compute the time derivative of polarization $\partial_t P_{y'}(z'_{\alpha,\mu}, t_{\beta+1})$ ($\alpha = 1, \dots N_1$, $\mu = 2 \dots N_2$) at time $t_{\beta+1}$ and at all other locations $\{z'_{\alpha,\mu}\}$ of the MEs domain;
- Thus, at time $t_{\beta+1}$ we have $\partial_t P_{y'}(z'_{\alpha,1}, t_{\beta+1})$, computed using the TDSEs, and $\partial_t P_{y'}(z'_{\alpha,\mu}, t_{\beta+1})$ ($\mu = 2 \dots N_2$), computed using the polarization evolution equation. We use these data to solve the MEs (1a) and (1b) in the domain at time $t_{\beta+1}$.

Finally we note that in the case of linearly polarized pulses, it is easy to generalize (20) including higher order nonlinearities:

$$
\begin{aligned}
(23) \quad & a(E_{y'}) := 1 + 4\pi(v_g/c)^2(3\chi^{(3)}E_{y'}^2 + 5\chi^{(5)}E_{y'}^4 + 7\chi^{(7)}E_{y'}^6 + \dots), \\
& b(E_{y'}) := E_{y'}(v_g/c)^2(6\chi^{(3)} + 20\chi^{(5)}E_{y'}^2 + 42\chi^{(7)}E_{y'}^4 + \dots), \\
& g(E_{y'}) := 4\pi(v_g/c)^2(\chi^{(1)} + 3\chi^{(3)}E_{y'}^2 + 5\chi^{(5)}E_{y'}^4 + 7\chi^{(7)}E_{y'}^6 + \dots) = \\
& \quad\quad\quad = 4\pi(v_g/c)^2\chi^{(1)} + [a(E_{y'})]^{-1} - 1.
\end{aligned}
$$

3. Existence and uniqueness of the weak solutions for the MASP models.
In this section, we study the well-posedness of the MASP models. We start the analysis with the MASP model, see Remark 2.1, which we will also refer to as the "pure" MASP model (in contrast to the "enriched" model). We base our proof on the results that were established earlier for the Schrödinger equation [4, 20, 27] and the Maxwell-Schrödinger model [28], which does not include the description of the plasma effects. Then, we discuss the existence and regularity of solutions to the model supplemented by the evolution equations for polarization (9), and for the free electrons density (17).

3.1. Pure MASP Model. Let $(\mathbf{E}_0, \mathbf{B}_0, \mathbf{J}_0, \overline{\psi}_0)^T$ be the initial data of the equations (1a), (1b), (2b), and (5), where $\overline{\psi}_0 = (\psi_{0,1} \dots \psi_{0,m})^T$, and m is the total number of cells in the gas region. We suppose that $\mathbf{E}_0, \mathbf{B}_0, \mathbf{J}_0$ belong to $\left(H^1(\Omega)\right)^3$, where

- $\Omega \subset \mathbb{R}^3$ is a bounded spatial domain for Maxwell's equations with a smooth boundary $\partial\Omega$ where Dirichlet zero BCs be imposedposed for $\mathbf{E}, \mathbf{B}, \mathbf{J}$. In other words, we assume that the electromagnetic pulse remains always inside the domain Ω, so that for all time the flux of the Poynting vector $\mathbf{S} = \dfrac{c}{4\pi}\mathbf{E} \times \mathbf{B}$ (recall, in our case $\mathbf{B} \equiv \mathbf{H}$) at the boundary $\partial\Omega$ is zero as well;
- $H^1(\Omega)$ denotes the Sobolev space $W^{1,2}(\Omega)$ [47]:

$$
(24) \quad\quad H^1(\Omega) = \{v \in L^2(\Omega) \mid \partial_{x_i} v_{\mathcal{D}'} \in L^2(\Omega), \quad i = 1, 2, 3\},
$$

where the derivative $\partial_{x_i} v_{\mathcal{D}'}$ is defined in the distributional (weak) sense, and L^p ($1 \le p < +\infty$) denote the Lebesgue spaces. Further in this section, we will omit the symbol $\mathcal{D}'$ on the derivatives, for the sake of simplicity of the notation.

In the Born-Oppenheimer approximation the distance between nuclei $R_0 > 0$ is a fixed parameter of the wavefunctions. We suppose that $\overline{\psi}_0 \in \left(H^1(\mathbb{R}^3) \cap H_1(\mathbb{R}^3)\right)^m$, where the norm of the Sobolev space $H^1(\mathbb{R}^3)$ reads

$$
(25) \quad\quad \|\psi\|_{H^1}^2 = \int_{\mathbb{R}^3} \left(|\psi(\mathbf{x}, R_0)|^2 + \sum_{i=1}^3 |\partial_{x_i}\psi(\mathbf{x}, R_0)|^2\right)d\mathbf{x}.
$$

The norm of *another* Sobolev space H_1 (with *low* index), which is the image of H^1 (with *upper* index) under the Fourier transform [4, 47], is defined as:

$$\|\psi\|_{H_1}^2 = \int_{\mathbb{R}^3} (1 + |(\mathbf{x}, \mathbf{R}_0)|^2) |\psi(\mathbf{x}, R_0)|^2 d\mathbf{x}, \tag{26}$$

where $|(\mathbf{x}, \mathbf{R}_0)|^2 := |\mathbf{x} - \mathbf{R}_0|^2 = |\mathbf{x} - \mathbf{e}_0 R_0|^2$ with unit vector $\mathbf{e}_0$ that defines the orientation of the molecule in plane (x, y).

Now we extend the Existence and Uniqueness Theorem [28], referred to solutions of the Maxwell-Shrödinger (MS) model, to the case of MASP model.

THEOREM 3.1. *Suppose that* $(\mathbf{E}_0, \mathbf{B}_0, \mathbf{J}_0) \in \left(H^1(\Omega)\right)^3 \times \left(H^1(\Omega)\right)^3 \times \left(H^1(\Omega)\right)^3$, $\overline{\psi}_0 \in (H^1 \cap H_1)^m$, $R_0 > 0$ *is a constant for all* $t \in \mathbb{R}_+$ *and* $\mathcal{N} \in C_0^\infty(\Omega)$. *Suppose that on the smooth boundary* $\partial\Omega$ *zero Dirichlet BCs are imposed on vectors* $\mathbf{E}, \mathbf{B}, \mathbf{J}$ *for all* $t \in \mathbb{R}_+$. *Then there exists a time* $T > 0$, *and a unique solution* $(\mathbf{E}, \mathbf{B}, \mathbf{J}, \overline{\psi}) \in \left(L^\infty(0, T; (H^1(\Omega))^3) \cap H^1(0, T; (L^2(\Omega))^3)\right)^3 \times L^\infty(0, T; (H^1 \cap H_1)^m)$ *to Equations* (1a), (1b), (2b), *and* (5).

In order to prove this theorem, we should prove several important intermediate results. The first lemma follows closely [28] and [4].

LEMMA 3.2. *Suppose that* $\mathbf{E}(\mathbf{x}', \cdot) \in L^\infty(0, T)$ *and* $\partial_t \mathbf{E}(\mathbf{x}', \cdot) \in L^1(0, T)$ *for* $\mathbf{x}'$ *fixed in* Ω. *We assume that* $R_0 > 0$ *is fixed for all* $t \in \mathbb{R}_+$. *Then for all* $\psi_{0,i} \in H^1 \cap H_1$, *there exists* $\psi_i \in L^\infty(0, T; H^1 \cap H_1)$ *solution to the Schrödinger equation* (2b), *and there exists a constant* $C_T > 0$ *such that*

$$\|\psi_i\|_{L^\infty(0,T;H^1 \cap H_1)} \le C_T \|\psi_{0,i}\|_{H^1 \cap H_1}.$$

The proof can be found in [28].

The next lemma from [28] generalizes the result of Lemma 3.2, on the vector-valued function $\overline{\psi} = (\psi_1 \ldots \psi_m)^T$:

LEMMA 3.3 (Lorin et al. [28]). *Suppose given* $\mathbf{E}(\mathbf{x}', \cdot) \in L^\infty(0, T)$ *and* $\partial_t \mathbf{E}(\mathbf{x}', \cdot) \in L^1(0, T)$, *for* $\mathbf{x}'$ *fixed in* Ω. *Then there exists* $C_T > 0$, *such that for all* $\overline{\psi}_0 \in (H^1 \cap H_1)^m$ *there exists a solution* $\overline{\psi} \in L^\infty(0, T; (H^1 \cap H_1)^m)$ *and*

$$\|\overline{\psi}\|_{L^\infty(0,T;(H^1 \cap H_1)^m)} \le C_T \|\overline{\psi}_0\|_{(H^1 \cap H_1)^m}.$$

Proof. It follows from the previous lemma. $\qquad\blacksquare$

LEMMA 3.4 (Lorin et al.[28]). *For all* $T > 0$, *and* $\overline{\psi} \in L^\infty(0, T; (H^1 \cap H_1)^m)$, $\mathbf{P} \in L^\infty(0, T; (\mathcal{C}_0^\infty)^3)$.

Proof. Recall that χ_{Ω_i}, $\mathcal{N}$ belong to $\mathcal{C}_0^\infty(\Omega)$ and $\psi_i \in L^\infty(0, T; H^1 \cap H_1)$, for all $i = 1, \ldots, m$, we then deduce that

$$t \mapsto \int_{\mathbb{R}^3 \times \mathbb{R}_+} \psi_i^*(R_0, \mathbf{x}, t) \mathbf{x} \psi_i(R_0, \mathbf{x}, t) \in L^\infty(0, T).$$

In particular for all $i = 1, \ldots, m$, as ψ_i belongs to $H^1 \cap H_1$, and the integral is defined. Finally, by definition of polarization (2a):

$$\mathbf{P}(\mathbf{x}', t) = -\mathcal{N}(\mathbf{x}') \sum_{i=1}^m \chi_{\Omega_i}(\mathbf{x}') \int_{R^3} \psi_i^*(R_0, \mathbf{x}, t) \mathbf{x} \psi_i(R_0, \mathbf{x}, t) d\mathbf{x} dR_0,$$

which concludes the proof. $\qquad\blacksquare$

LEMMA 3.5 (Lorin et al.[28]).   *For $\mathbf{x}'$ fixed in Ω and $T > 0$, $\partial_t \mathbf{P}(\mathbf{x}', \cdot) \in L^\infty(0, T)$ and $\partial_t(\nabla \cdot \mathbf{P}(\mathbf{x}', \cdot)) \in L^\infty(0, T)$.*

Proof. First, we observe that $\partial_t \mathbf{P}(\mathbf{x}', t) = \mathcal{N}(\mathbf{x}') \sum_{i=1}^{m} \partial_t \mathbf{P}_i(\mathbf{x}', t)$, where

$$\partial_t \mathbf{P}_i(\mathbf{x}', t) = \chi_{\Omega_i}(\mathbf{x}') \int_{R^3} \partial_t \psi_i^*(R_0, \mathbf{x}, t) \mathbf{x} \psi_i(R_0, \mathbf{x}, t) d\mathbf{x} dR_0 +$$
$$+ \chi_{\Omega_i}(\mathbf{x}') \int_{R^3} \psi_i^*(R_0, \mathbf{x}, t) \mathbf{x} \partial_t \psi_i(R_0, \mathbf{x}, t) d\mathbf{x} dR_0.$$

As $\psi_i \in L^\infty(0, T; H^1 \cap H_1)$ and $\chi_{\Omega_i}, \mathcal{N} \in \mathcal{C}_0^\infty(\Omega)$ then $\partial_t \mathbf{P}_i \in L^\infty(0, T)$ for all $i = 1, \ldots, m$, hence $\partial_t \mathbf{P} \in L^\infty(0, T)$. Also as, according to Lemma 3.4, $\nabla \cdot \mathbf{P}(\cdot, t) \in \mathcal{C}_0^\infty(\Omega)$ at t fixed, we also have that $\partial_t(\nabla \cdot \mathbf{P})(\mathbf{x}', \cdot) \in L^\infty(0, T)$. $\square$

LEMMA 3.6. *Suppose given $\mathcal{N}_{e0} \in \mathcal{C}_0^\infty$, then for all $T > 0$, and $\overline{\psi} \in L^\infty(0, T; (H^1 \cap H_1)^m)$, $\mathcal{N}_e \in L^\infty(0, T; \mathcal{C}_0^\infty)$.*

Proof. We know that $\mathcal{N}$ and χ_{Ω_i} being to $\mathcal{C}_0^\infty$. Following Equations (6), (7), the expression for density of free electron $\mathcal{N}_e(\mathbf{x}', t)$ at different $\mathbf{x}'$ reads

$$\mathcal{N}_e(\mathbf{x}', t) = \mathcal{N}_{e0}(\mathbf{x}') + \mathcal{N}(\mathbf{x}') \sum_{i=1}^{m} \chi_{\Omega_i}(\mathbf{x}') \Big(1 - \int_{\Omega_i} |\psi_i(R_0, \mathbf{x}', t)|^2 d\mathbf{x}\Big) dR_0,$$

which proves the lemma. $\square$

LEMMA 3.7. *Suppose that $\mathbf{E}(t)|_{\partial\Omega} = \mathbf{B}(t)|_{\partial\Omega} = \mathbf{0} \in \mathbb{R}^3$, then for all $T > 0$ and $\Omega \subset \mathbb{R}^3$*

(27)
$$\|\mathbf{E}(\cdot, T)\|^2_{\left(L^2(\Omega)\right)^3} + \|\mathbf{B}(\cdot, T)\|^2_{\left(L^2(\Omega)\right)^3} = \|\mathbf{E}_0(\cdot)\|^2_{\left(L^2(\Omega)\right)^3} + \|\mathbf{B}_0(\cdot)\|^2_{\left(L^2(\Omega)\right)^3} -$$
$$- 8\pi \int_0^T \int_\Omega \mathbf{E}(\mathbf{x}', t) \cdot \partial_t \mathbf{P}(\mathbf{x}', t) d\mathbf{x}' dt - 8\pi \int_0^T \int_\Omega \mathbf{E}(\mathbf{x}', t) \cdot \mathbf{J}(\mathbf{x}', t) d\mathbf{x}' dt,$$

and
(28)
$$\|\nabla\cdot\mathbf{E}(\cdot, T)\|^2_{L^2(\Omega)} = \|\nabla\cdot\mathbf{E}_0(\cdot)\|^2_{L^2(\Omega)} - 8\pi \int_0^T \int_\Omega \nabla\cdot\mathbf{E}(\mathbf{x}', t)\partial_t\nabla\cdot\mathbf{P}(\mathbf{x}', t)d\mathbf{x}' dt -$$
$$- 8\pi \int_0^T \int_\Omega \nabla\cdot\mathbf{E}(\mathbf{x}', t)\nabla\cdot\mathbf{J}(\mathbf{x}', t)d\mathbf{x}' dt.$$

Proof. We respectively use Ampere-Maxwell's (1a) and Faraday-Maxwell's (1b) laws: We take the scalar products of (1a) with $\mathbf{E}$, and (1b) with $\mathbf{B}$ that result in

(29)
$$\mathbf{E}(\mathbf{x}', t) \cdot \partial_t \mathbf{E}(\mathbf{x}', t) = c\mathbf{E}(\mathbf{x}', t) \cdot [\nabla \times \mathbf{B}(\mathbf{x}', t)] -$$
$$- 4\pi \mathbf{E}(\mathbf{x}', t) \cdot \partial_t \mathbf{P}(\mathbf{x}', t) - 4\pi \mathbf{E}(\mathbf{x}', t) \cdot \mathbf{J}(\mathbf{x}', t),$$
$$\mathbf{B}(\mathbf{x}', t) \cdot \partial_t \mathbf{B}(\mathbf{x}', t) = -c\mathbf{B}(\mathbf{x}', t) \cdot [\nabla \times \mathbf{E}(\mathbf{x}', t)].$$

Noticing that in the LHSs $\mathbf{E}(\mathbf{x}', t)\cdot\partial_t\mathbf{E}(\mathbf{x}', t) = \partial_t\mathbf{E}^2(\mathbf{x}', t)/2$ and $\mathbf{B}(\mathbf{x}', t)\cdot\partial_t\mathbf{B}(\mathbf{x}', t) = \partial_t\mathbf{B}^2(\mathbf{x}', t)/2$, so that we obtain after integration over $(0, T) \times \Omega$:

$$\int_0^T \int_\Omega \mathbf{E}(\mathbf{x}', t) \cdot \partial_t \mathbf{E}(\mathbf{x}', t) d\mathbf{x}' dt = \frac{1}{2}\big(\|\mathbf{E}(\cdot, T)\|^2_{\left(L^2(\Omega)\right)^3} - \|\mathbf{E}_0(\cdot)\|^2_{\left(L^2(\Omega)\right)^3}\big),$$
$$\int_0^T \int_\Omega \mathbf{B}(\mathbf{x}', t) \cdot \partial_t \mathbf{B}(\mathbf{x}', t) d\mathbf{x}' dt = \frac{1}{2}\big(\|\mathbf{B}(\cdot, T)\|^2_{\left(L^2(\Omega)\right)^3} - \|\mathbf{B}_0(\cdot)\|^2_{\left(L^2(\Omega)\right)^3}\big).$$

We add the expressions (29) using that $\nabla \cdot [\mathbf{E} \times \mathbf{B}] = \mathbf{B} \cdot [\nabla \times \mathbf{E}] - \mathbf{E} \cdot [\nabla \times \mathbf{B}]$, and integrating over $(0,T) \times \Omega$. Finally, using the divergence theorem, we deduce (27).

Now we apply the operator ∇ to both sides of (1a). Since the divergence of the curl is 0, we obtain the equation

$$(30) \qquad \partial_t \nabla \cdot \mathbf{E}(\mathbf{x}', t) = -4\pi \partial_t \nabla \cdot \mathbf{P}(\mathbf{x}', t) - 4\pi \nabla \cdot \mathbf{J}(\mathbf{x}', t).$$

We take the product of the scalar equation (30) with a scalar $\nabla \cdot \mathbf{E}$ and again integrate over $(0,T) \times \Omega$ resulting in (28). $\qquad \square$

LEMMA 3.8. *Suppose that* $\mathbf{E}(t)|_{\partial\Omega} = \mathbf{B}(t)|_{\partial\Omega} = \mathbf{0} \in \mathbb{R}^3$, *then for all* $T > 0$ *and* $\Omega \subset \mathbb{R}^3$

$$
\begin{aligned}
(31) \quad & \|\partial_t \mathbf{E}(\cdot, T)\|^2_{\left(L^2(\Omega)\right)^3} + c^2 \|\nabla \times \mathbf{E}(\cdot, T)\|^2_{\left(L^2(\Omega)\right)^3} = \|\partial_t \mathbf{E}_0(\cdot)\|^2_{\left(L^2(\Omega)\right)^3} + \\
& + \|\nabla \times \mathbf{E}_0(\cdot)\|^2_{\left(L^2(\Omega)\right)^3} - 8\pi \int_0^T \int_\Omega \partial_t \mathbf{E}(\mathbf{x}', t) \cdot \partial_t^2 \mathbf{P}(\mathbf{x}', t) d\mathbf{x}' dt - \\
& - 8\pi \int_0^T \int_\Omega \partial_t \mathbf{E}(\mathbf{x}', t) \cdot \partial_t \mathbf{J}(\mathbf{x}', t) d\mathbf{x}' dt,
\end{aligned}
$$

and

$$
\begin{aligned}
(32) \quad & \|\partial_t \mathbf{B}(\cdot, T)\|^2_{\left(L^2(\Omega)\right)^3} + c^2 \|\nabla \times \mathbf{B}(\cdot, T)\|^2_{\left(L^2(\Omega)\right)^3} = \|\partial_t \mathbf{B}_0(\cdot)\|^2_{\left(L^2(\Omega)\right)^3} + \\
& + \|\nabla \times \mathbf{B}_0(\cdot)\|^2_{\left(L^2(\Omega)\right)^3} + 8\pi c \int_0^T \int_\Omega \partial_t \mathbf{B}(\mathbf{x}', t) \cdot \partial_t [\nabla \times \mathbf{P}(\mathbf{x}', t)] d\mathbf{x}' dt + \\
& + 8\pi c \int_0^T \int_\Omega \partial_t \mathbf{B}(\mathbf{x}', t) \cdot [\nabla \times \mathbf{J}(\mathbf{x}', t)] d\mathbf{x}' dt.
\end{aligned}
$$

Proof. We differentiate (1a) in time and then multiply both sides by $\partial_t \mathbf{E}$. We note that

$$
\partial_t \mathbf{E} \cdot \partial_t^2 \mathbf{E} = \frac{1}{2} \partial_t (\partial_t \mathbf{E} \cdot \partial_t \mathbf{E}) = \frac{1}{2} \partial_t |\partial_t \mathbf{E}|^2,
$$
$$
\partial_t \mathbf{E} \cdot [\nabla \times [\nabla \times \mathbf{E}]] = \nabla \cdot [[\nabla \times \mathbf{E}] \times \partial_t \mathbf{E}] + [\nabla \times \mathbf{E}] \cdot [\nabla \times \partial_t \mathbf{E}] =
$$
$$
= \nabla \cdot [[\nabla \times \mathbf{E}] \times \partial_t \mathbf{E}] + \frac{1}{2} \partial_t |\nabla \times \mathbf{E}|^2.
$$

We integrate the equation over $(0,T) \times \Omega$, apply the divergence theorem and obtain (31). Similarly, by differentiation (1b) in time, then by multiplication by $\partial_t \mathbf{B}$ and finally by integration over $(0,T) \times \Omega$ we come to (32). $\qquad \square$

LEMMA 3.9. *For all* $T > 0$,

$$
\begin{aligned}
(33) \quad & \|\mathbf{J}(\cdot, T)\|^2_{\left(L^2(\Omega)\right)^3} = \|\mathbf{J}_0(\cdot)\|^2_{\left(L^2(\Omega)\right)^3} - 2\nu_e \int_0^T \|\mathbf{J}(\cdot, t)\|^2_{\left(L^2(\Omega)\right)^3} dt + \\
& + 2 \int_0^T \int_\Omega \mathcal{N}_e(\mathbf{x}', t) \mathbf{J}(\mathbf{x}', t) \cdot \mathbf{E}(\mathbf{x}', t) d\mathbf{x}' dt
\end{aligned}
$$

and

$$
\begin{aligned}
(34) \quad & \|\partial_t \mathbf{J}(\cdot, T)\|^2_{\left(L^2(\Omega)\right)^3} = \|\partial_t \mathbf{J}_0(\cdot)\|^2_{\left(L^2(\Omega)\right)^3} - 2\nu_e \int_0^T \|\partial_t \mathbf{J}(\cdot, t)\|^2_{\left(L^2(\Omega)\right)^3} dt + \\
& + 2 \int_0^T \int_\Omega \mathcal{N}_e(\mathbf{x}', t) \partial_t \mathbf{J}(\mathbf{x}', t) \cdot \partial_t \mathbf{E}(\mathbf{x}', t) d\mathbf{x}' dt + \\
& + 2 \int_0^T \int_\Omega \partial_t \mathcal{N}_e(\mathbf{x}', t) \partial_t \mathbf{J}(\mathbf{x}', t) \cdot \mathbf{E}(\mathbf{x}', t) d\mathbf{x}' dt
\end{aligned}
$$

and

$$\|\nabla \cdot \mathbf{J}(\cdot, T)\|^2_{L^2(\Omega)} = \|\nabla \cdot \mathbf{J}_0(\cdot)\|^2_{L^2(\Omega)} - 2\nu_e \int_0^T \|(\nabla \cdot \mathbf{J})(\cdot, t)\|^2_{L^2(\Omega)} dt +$$

(35)
$$+ 2 \int_0^T \int_\Omega \nabla \mathcal{N}_e(\mathbf{x}', t) \cdot \mathbf{E}(\mathbf{x}', t) \nabla \cdot \mathbf{J}(\mathbf{x}', t) d\mathbf{x}' dt +$$

$$+ 2 \int_0^T \int_\Omega \mathcal{N}_e(\mathbf{x}', t) \nabla \cdot \mathbf{E}(\mathbf{x}', t) \nabla \cdot \mathbf{J}(\mathbf{x}', t) d\mathbf{x}' dt$$

and finally
(36)

$$\|\nabla \times \mathbf{J}(\cdot, T)\|^2_{\left(L^2(\Omega)\right)^3} = \|\nabla \times \mathbf{J}_0(\cdot)\|^2_{\left(L^2(\Omega)\right)^3} - 2\nu_e \int_0^T \|(\nabla \times \mathbf{J})(\cdot, t)\|^2_{\left(L^2(\Omega)\right)^3} dt +$$

$$+ 2 \int_0^T \int_\Omega [\nabla \mathcal{N}_e(\mathbf{x}', t) \times \mathbf{E}(\mathbf{x}', t)] \cdot [\nabla \times \mathbf{J}(\mathbf{x}', t)] d\mathbf{x}' dt +$$

$$+ 2 \int_0^T \int_\Omega \mathcal{N}_e(\mathbf{x}', t) [\nabla \times \mathbf{E}(\mathbf{x}', t)] \cdot [\nabla \times \mathbf{J}(\mathbf{x}', t)] d\mathbf{x}' dt.$$

Proof. We take the scalar product of (5) with $\mathbf{J}$

$$\frac{1}{2} \partial_t |\mathbf{J}(\mathbf{x}', t)|^2 = -\nu_e |\mathbf{J}(\mathbf{x}', t)|^2 + \mathcal{N}_e(\mathbf{x}', t) \mathbf{J}(\mathbf{x}', t) \cdot \mathbf{E}(\mathbf{x}', t).$$

Integrating over $(0, T)$, gives (33). To prove (34), we differentiate Equation (5) in time, then we take the scalar product of both parts with $\partial_t \mathbf{J}$, and integrate over $(0, T)$.

By applying $\nabla \cdot$ on (5), and then integrating over $(0, T)$ with $\nabla \cdot \mathbf{J}$, we deduce (35). Finally, by applying $\nabla \times$ on (5), and then integrating over $(0, T)$ with $\nabla \times \mathbf{J}$, we deduce (36). □

Remark 3.10. With a view of proper management of the physical variable dimensions in the following lemmas, we should make a remark. Recall that we use atomic units for all the equations, so that from MEs (1a) and (1b) we can conclude that $\dim(\mathbf{E}) = \mathrm{T} \dim(\mathbf{J})$, where T is the symbol for the time dimension. Taking into account Drude's model (5), we can see that $\dim(\mathcal{N}_e) = \mathrm{T}^{-2}$. In the following, we introduce a constant $\eta > 0$, having the dimension of time, $\dim(\eta) = \mathrm{T}$.

LEMMA 3.11. *There exists a constant $C > 0$ such that for all time $T > 0$*

$$(37) \quad \sup_{0 \le t \le T} \|\mathbf{E}(\cdot, t)\|^2_{(H^1(\Omega))^3} + \sup_{0 \le t \le T} \|\mathbf{B}(\cdot, t)\|^2_{(H^1(\Omega))^3} + \eta^2 \sup_{0 \le t \le T} \|\mathbf{J}(\cdot, t)\|^2_{(H^1(\Omega))^3} \le C.$$

Proof. From the result (27) of Lemma 3.7 we have for all $t \in (0, T]$

$$\|\mathbf{E}(\cdot, T)\|^2_{\left(L^2(\Omega)\right)^3} + \|\mathbf{B}(\cdot, T)\|^2_{\left(L^2(\Omega)\right)^3} \le \|\mathbf{E}_0(\cdot)\|^2_{\left(L^2(\Omega)\right)^3} + \|\mathbf{B}_0(\cdot)\|^2_{\left(L^2(\Omega)\right)^3} +$$

$$+ 8\pi \int_0^T \int_\Omega |\mathbf{E}(\mathbf{x}', t) \cdot \partial_t \mathbf{P}(\mathbf{x}', t)| d\mathbf{x}' dt + 8\pi \int_0^T \int_\Omega |\mathbf{E}(\mathbf{x}', t) \cdot \mathbf{J}(\mathbf{x}', t)| d\mathbf{x}' dt \le$$

$$\le \|\mathbf{E}_0(\cdot)\|^2_{\left(L^2(\Omega)\right)^3} + \|\mathbf{B}_0(\cdot)\|^2_{\left(L^2(\Omega)\right)^3} + 8\pi\eta^{-1} \int_0^T \|\mathbf{E}(\cdot, t)\|^2_{\left(L^2(\Omega)\right)^3} dt +$$

$$4\pi\eta \int_0^T \|\partial_t \mathbf{P}(\cdot, t)\|^2_{\left(L^2(\Omega)\right)^3} dt + 4\pi\eta \int_0^T \|\mathbf{J}(\cdot, t)\|^2_{\left(L^2(\Omega)\right)^3} dt.$$

Similarly from (28):

$$\|\nabla\cdot\mathbf{E}(\cdot,T)\|_{L^2(\Omega)}^2 \le \|\nabla\cdot\mathbf{E}_0(\cdot)\|_{L^2(\Omega)}^2 + 8\pi \int_0^T \int_\Omega |\nabla\cdot\mathbf{E}(\mathbf{x}',t)\partial_t\nabla\cdot\mathbf{P}(\mathbf{x}',t)|d\mathbf{x}'dt+$$

$$+8\pi \int_0^T \int_\Omega |\nabla\cdot\mathbf{E}(\mathbf{x}',t)\nabla\cdot\mathbf{J}(\mathbf{x}',t)|d\mathbf{x}'dt \le \|\nabla\cdot\mathbf{E}_0(\cdot)\|_{L^2(\Omega)}^2+$$

$$+8\pi\eta^{-1} \int_0^T \|\nabla\cdot\mathbf{E}(\cdot,t)\|_{L^2(\Omega)}^2 dt + 4\pi\eta \int_0^T \|\partial_t\nabla\cdot\mathbf{P}(\cdot,t)\|_{L^2(\Omega)}^2 dt+$$

$$+4\pi\eta \int_0^T \|\nabla\cdot\mathbf{J}(\cdot,t)\|_{L^2(\Omega)}^2 dt.$$

From Lemma 3.6 and (33) of Lemma 3.9, we have for all $t \in (0, T]$

$$\|\mathbf{J}(\cdot,T)\|_{\left(L^2(\Omega)\right)^3}^2 \le \|\mathbf{J}_0(\cdot)\|_{\left(L^2(\Omega)\right)^3}^2 + 2\nu_e \int_0^T \|\mathbf{J}(\cdot,t)\|_{\left(L^2(\Omega)\right)^3}^2 dt+$$

$$+2\int_0^T \int_\Omega \mathcal{N}_e(\mathbf{x}',t)|\mathbf{J}(\mathbf{x}',t)\cdot\mathbf{E}(\mathbf{x}',t)|d\mathbf{x}'dt \le \|\mathbf{J}_0(\cdot)\|_{\left(L^2(\Omega)\right)^3}^2+$$

$$+(2\nu_e + \eta^{-1})\int_0^T \|\mathbf{J}(\cdot,t)\|_{\left(L^2(\Omega)\right)^3}^2 dt + \eta \sup_{\Omega,[0,T]}\mathcal{N}_e^2(\mathbf{x}',t)\int_0^T \|\mathbf{E}(\cdot,t)\|_{\left(L^2(\Omega)\right)^3}^2 dt,$$

and with Lemma 3.6 and (35)

$$\|\nabla\cdot\mathbf{J}(\cdot,T)\|_{L^2(\Omega)}^2 \le \|\nabla\cdot\mathbf{J}_0(\cdot)\|_{L^2(\Omega)}^2 + 2\nu_e \int_0^T \int_\Omega |(\nabla\cdot\mathbf{J})(\mathbf{x}',t)|^2 d\mathbf{x}'dt+$$

$$+2\int_0^T \int_\Omega |\nabla\mathcal{N}_e(\mathbf{x}',t)\cdot\mathbf{E}(\mathbf{x}',t)\nabla\cdot\mathbf{J}(\mathbf{x}',t)|d\mathbf{x}'dt+$$

$$+2\int_0^T \int_\Omega |\mathcal{N}_e(\mathbf{x}',t)\nabla\cdot\mathbf{E}(\mathbf{x}',t)\nabla\cdot\mathbf{J}(\mathbf{x}',t)|d\mathbf{x}'dt \le \|\nabla\cdot\mathbf{J}_0(\cdot)\|_{L^2(\Omega)}^2+$$

$$+2(\nu_e + \eta^{-1})\int_0^T \|(\nabla\cdot\mathbf{J})(\cdot,t)\|_{L^2(\Omega)}^2 dt+$$

$$+\eta \sup_{\Omega,[0,T]}(\nabla\mathcal{N}_e(\mathbf{x}',t))^2 \int_0^T \|\mathbf{E}(\cdot,t)\|_{L^2(\Omega)}^2 dt+$$

$$+\eta \sup_{\Omega,[0,T]}\mathcal{N}_e^2(\mathbf{x}',t)\int_0^T \|\nabla\cdot\mathbf{E}(\cdot,t)\|_{L^2(\Omega)}^2 d\mathbf{x}'dt.$$

Combining the first and third inequalities, we get:

$$(38) \quad \begin{aligned} &\|\mathbf{E}(\cdot,T)\|_{\left(L^2(\Omega)\right)^3}^2 + \|\mathbf{B}(\cdot,T)\|_{\left(L^2(\Omega)\right)^3}^2 + \eta^2\|\mathbf{J}(\cdot,T)\|_{\left(L^2(\Omega)\right)^3}^2 \le \\ &\le \|\mathbf{E}_0(\cdot)\|_{\left(L^2(\Omega)\right)^3}^2 + \|\mathbf{B}_0(\cdot)\|_{\left(L^2(\Omega)\right)^3}^2 + \eta^2\|\mathbf{J}_0(\cdot)\|_{\left(L^2(\Omega)\right)^3}^2+ \\ &+(8\pi\eta^{-1} + \eta^3 \sup_{\Omega,[0,T]}\mathcal{N}_e^2(\mathbf{x}',t))\int_0^T \|\mathbf{E}(\cdot,t)\|_{\left(L^2(\Omega)\right)^3}^2 dt+ \\ &+(4\pi\eta + 2\nu_e\eta^2 + \eta)\int_0^T \|\mathbf{J}(\cdot,t)\|_{\left(L^2(\Omega)\right)^3}^2 dt + 4\pi\eta \int_0^T \|\partial_t\mathbf{P}(\cdot,t)\|_{\left(L^2(\Omega)\right)^3}^2 dt. \end{aligned}$$

Identically for the second and fourth inequalities:
(39)
$$
\begin{aligned}
\|\nabla\cdot\mathbf{E}(\cdot,T)\|^2_{L^2(\Omega)} + \eta^2\|\nabla\cdot\mathbf{J}(\cdot,T)\|^2_{L^2(\Omega)} &\leq \|\nabla\cdot\mathbf{E}_0(\cdot)\|^2_{L^2(\Omega)} + \eta^2\|\nabla\cdot\mathbf{J}_0(\cdot)\|^2_{L^2(\Omega)} + \\
&+ (8\pi\eta^{-1} + \eta^3\sup_{\Omega,[0,T]}\mathcal{N}_e^2(\mathbf{x}',t))\int_0^T\|\nabla\cdot\mathbf{E}(\cdot,t)\|^2_{L^2(\Omega)}dt + \\
&+ (4\pi\eta + 2\nu_e\eta^2 + 2\eta)\int_0^T\|\nabla\cdot\mathbf{J}(\cdot,t)\|^2_{L^2(\Omega)}dt + \\
+\eta^3\sup_{\Omega,[0,T]}(\nabla\mathcal{N}_e(\mathbf{x}',t))^2\int_0^T\|\mathbf{E}(\cdot,t)\|^2_{L^2(\Omega)}dt &+ 4\pi\eta\int_0^T\|\partial_t\nabla\cdot\mathbf{P}(\cdot,t)\|^2_{L^2(\Omega)}dt.
\end{aligned}
$$

In addition to (39), we recall that $\nabla\cdot\mathbf{B}(\mathbf{x}',t)\equiv 0$. According to Lemmas 3.5 and 3.6, $\partial_t\mathbf{P}\in L^\infty(0,T;(\mathcal{C}_0^\infty)^3)$ and $\mathcal{N}_e(\mathbf{x}',t)\in L^\infty(0,T;\mathcal{C}_0^\infty)$, so using Grönwall's inequality we can confirm boundedness of the norms in the LHS of inequalities (38) and (39).

Similarly, using Lemma 3.8 and equations (34) and (36), we can conclude boundedness of the following combination of the norms:

$$
\begin{aligned}
\|\partial_t\mathbf{E}(\cdot,T)\|^2_{\left(L^2(\Omega)\right)^3} + c^2\|\nabla\times\mathbf{E}(\cdot,T)\|^2_{\left(L^2(\Omega)\right)^3} + \|\partial_t\mathbf{B}(\cdot,T)\|^2_{\left(L^2(\Omega)\right)^3} + \\
+ c^2\|\nabla\times\mathbf{B}(\cdot,T)\|^2_{\left(L^2(\Omega)\right)^3} + \eta^2\left\{\|\partial_t\mathbf{J}(\cdot,T)\|^2_{\left(L^2(\Omega)\right)^3} + c^2\|\nabla\times\mathbf{J}(\cdot,T)\|^2_{\left(L^2(\Omega)\right)^3}\right\}.
\end{aligned}
$$

From here we deduce (37). □

Proof. of Theorem 3.1. So far, we have proven that for all $T>0$, there exists a constant $C>0$ such that:

$$
\begin{aligned}
\|\mathbf{E}\|^2_{L^\infty\left(0,T;(H^1(\Omega))^3\right)\cap H^1\left(0,T;(L^2(\Omega))^3\right)} &+ \|\mathbf{B}\|^2_{L^\infty\left(0,T;(H^1(\Omega))^3\right)\cap H^1\left(0,T;(L^2(\Omega))^3\right)} + \\
+\eta^2\|\mathbf{J}\|^2_{L^\infty\left(0,T;(H^1(\Omega))^3\right)\cap H^1\left(0,T;(L^2(\Omega))^3\right)} &+ \mu\|\overline{\psi}\|_{L^\infty\left(0,T;(H^1\cap H_1)^m\right)} \leq C,
\end{aligned}
$$

where $\mu>0$ is a dimensional constant, such that $\dim(\mu)=\dim(\mathbf{E}^2)$. The boundness of the last term in the above inequality is a consequence of Lemma 3.2. Now as $L^\infty\left(0,T;(H^1(\Omega))^3\right)\times L^\infty\left(0,T;(H^1\cap H_1)^m\right)$ is compactly embedded in $L^2(\Omega\times(0,T])\times (L^2(\mathbb{R}^3))^m$ by Leray-Schauder's fixed point theorem, we deduce the existence of a solution for (1a), (1b), (2b), and (5). The approach is the same as described in [49]. It is based on the introduction of a continuous mapping derived from (1a), (1b), and (2b), which depends on a parameter $\lambda\in[0,1]$ and admits a fixed point in $L^2(\Omega\times(0,T])\times(L^2(\mathbb{R}^3))^m$ as verifying Leray-Schauder's theorem assumptions [33].

Uniqueness is proven by a classical process of introducing two solutions of the Cauchy problem (1a), (1b), and (2b): $(\mathbf{E}_1,\mathbf{B}_1,\mathbf{J}_1,\overline{\psi}_2)^T$ and $(\mathbf{E}_2,\mathbf{B}_2,\mathbf{J}_2,\overline{\psi}_2)^T$, and denoting their difference as $(\mathbf{E},\mathbf{B},\mathbf{J},\overline{\psi})^T := (\mathbf{E}_2-\mathbf{E}_1,\mathbf{B}_2-\mathbf{B}_1,\mathbf{J}_2-\mathbf{J}_1,\overline{\psi}_2-\overline{\psi}_1)^T$ with ICs $(\mathbf{E}(\cdot,0),\mathbf{B}(\cdot,0),\mathbf{J}(\cdot,0),\overline{\psi}(\cdot,0))^T = (\mathbf{0},\mathbf{0},\mathbf{0},\mathbf{0})^T$. As in Lemmas 3.2 and 3.7, see also for details [28], there exists a constant $C>0$ such that:

(40)
$$
\begin{aligned}
\frac{d}{dt}\Bigg\{\mu\|\overline{\psi}(t)\|^2_{(H^1\cap H_1)^m} + \int_\Omega\Big(\|\mathbf{E}(\mathbf{x}',t)\|^2_{\left(L^2(\Omega)\right)^3} + \\
+\|\mathbf{B}(\mathbf{x}',t)\|^2_{\left(L^2(\Omega)\right)^3} + \eta^2\|\mathbf{J}(\mathbf{x}',t)\|^2_{\left(L^2(\Omega)\right)^3}\Big)d\mathbf{x}'\Bigg\} \leq \\
C\Bigg\{\mu\|\overline{\psi}(t)\|^2_{(H^1\cap H_1)^m} + \int_\Omega\Big(\|\mathbf{E}(\mathbf{x}',t)\|^2_{\left(L^2(\Omega)\right)^3} + \\
+\|\mathbf{B}(\mathbf{x}',t)\|^2_{\left(L^2(\Omega)\right)^3} + \eta^2\|\mathbf{J}(\mathbf{x}',t)\|^2_{\left(L^2(\Omega)\right)^3}\Big)d\mathbf{x}'\Bigg\}.
\end{aligned}
$$

Using Grönwall's inequality we conclude $\left(\mathbf{E}(\cdot,t),\mathbf{B}(\cdot,t),\mathbf{J}(\cdot,t),\overline{\psi}(\cdot,t)\right)^T \equiv (\mathbf{0},\mathbf{0},\mathbf{0},\mathbf{0})^T$ for all $t > 0$. Moreover, the polarization is also unique, $\mathbf{P} = \mathbf{P}_2 - \mathbf{P}_1 \equiv \mathbf{0}$ for $t \geq 0$, as by definition:

$$\mathbf{P}(\mathbf{x}',t) = \mathcal{N}(\mathbf{x}')\sum_{i=1}^m \mathbf{P}_i(\mathbf{x}',t) =$$
$$= \mathcal{N}(\mathbf{x}')\sum_{i=1}^m \chi_{\Omega_i}(\mathbf{x}')\int_{\mathbb{R}^3\times\mathbb{R}_+} \mathbf{x}\big(|\psi_{i,2}(R_0,\mathbf{x},t)|^2 - |\psi_{i,1}(R_0,\mathbf{x},t)|^2\big)d\mathbf{x}dR_0,$$

and as $\overline{\psi}(\cdot,t) \equiv \mathbf{0}$ for all $t > 0$. □

The main practical consequence of Theorem 3.1 in the sense of numerical treatment of the model is the conservation in time of regularity of the solutions, which justifies the use of finite difference methods (FDM) for solving equations formed the MASP model [27, 28]. In addition, we note that the FDM is a natural choice as the geometry of the computational domains of the MEs and TDSEs are simple enough.

3.2. MASP Model Supplemented by Evolution Equations for Polarization and Free Electron Density. This part discusses the issue, whether we could still rely on the same regularity of solutions in case of the MASP model enriched by the evolution equations for polarization and free electrons density. Certainly, it is too complicated to prove the theorem of existence and uniqueness for the MASP model with embedded general evolution equation (21) which, moreover, is nonlinear. However, since we intend to use this equation in the regime of relatively weak nonlinearity (with purpose to obtain a correction to the solution of homogeneous equation), it makes sense to consider at least the MASP model complemented by the homogeneous wave equations for polarization vector :

$$\partial_t^2\mathbf{P} - v_g^2\triangle\mathbf{P} = 0, \tag{41}$$

with velocity v_g, considered as a constant. Note that if we apply the operator ∇ to both sides of (41) and recall that the divergence of the polarization vector equals to the density of the bound charges taken with opposite sign, $\nabla \cdot \mathbf{P} = -(\mathcal{N} - \mathcal{N}_e)$, we obtain the evolution equation for the free electron density:

$$\partial_t^2\mathcal{N}_e - v_g^2\triangle\mathcal{N}_e = 0, \tag{42}$$

while the afore-mentioned equation (17) describes one-directional wave only. To obtain (42), we recall that the gas density depends on spatial coordinate only, $\mathcal{N} = \mathcal{N}(\mathbf{x}')$, and we make an assumption that this dependence is close to constant, i.e. $\nabla\mathcal{N}(\mathbf{x}') = \mathbf{0}$ and $\triangle\mathcal{N}(\mathbf{x}') = 0$ for all $\mathbf{x}' \in \Omega$.

We intend to solve the system of equations (1a), (1b), (2b), (5), (41), and (42) subject to the initial data set $(\mathbf{E}_0,\mathbf{B}_0,\mathbf{J}_0,\psi_0,\mathbf{P}_0,\partial_t\mathbf{P}_0,\mathcal{N}_{e0},\partial_t\mathcal{N}_{e0})^T$. For simplicity, we assume that the bounded domain of Maxwell's equations Ω contains only *one* "subdomain" $\widetilde{\Omega}$ with a gas, which means that now $\psi_0 \equiv \psi_{0,1}$. Using these microscopic data, we can compute $\mathbf{P}(t)|_{\partial\widetilde{\Omega}}$, see (2a), and $\mathcal{N}(t)|_{\partial\widetilde{\Omega}}$ see (6), (7), and their time derivatives in the first cell of the gas region, i.e. on the boundary of the gas region. We suppose that initially *within the domain*, the polarization vector and free electron number density equal zero: $\mathbf{P}_0 = \mathbf{0} \in \mathbb{R}^3$, $\partial_t\mathbf{P}_0 = \mathbf{0} \in \mathbb{R}^3$, $\mathcal{N}_{e0} = 0 \in \mathbb{R}$, $\partial_t\mathcal{N}_{e0} = 0 \in \mathbb{R}$. This provides for wave equations (41) and (42) the initial-boundary value problems. Now we state the existence theorem for the supplemented MASP model.

THEOREM 3.12. *Suppose that* $(\mathbf{E}_0, \mathbf{B}_0, \mathbf{J}_0) \in \left(H^1(\Omega)\right)^3 \times \left(H^1(\Omega)\right)^3 \times \left(H^1(\Omega)\right)^3$, $\psi_0 \in (H^1 \cap H_1)$, $R_0 > 0$ *is a constant for all* $t \in \mathbb{R}_+$ *and* $\mathcal{N} \in C_0^\infty(\Omega)$. *Suppose that on the smooth boundary* $\partial\Omega$ *zero Dirichlet BCs are imposed for vectors* $\mathbf{E}, \mathbf{B}, \mathbf{J}$, $\mathbf{P}$ *for all* $t \in \mathbb{R}_+$. *In addition, on the smooth boundary* $\partial\widetilde{\Omega}$ *of the gas region the values of* $\mathbf{P}(t)\big|_{\partial\widetilde{\Omega}}$, $\mathcal{N}_e(t)\big|_{\partial\widetilde{\Omega}}$ *are computed via* $\psi(R_0, \mathbf{x}, t)$ *from* (2b), (6), *and* (7) *with* $m = 1$, *while for* $t = 0$ $(\mathbf{P}_0, \partial_t\mathbf{P}_0, \mathcal{N}_{e0}, \partial_t\mathcal{N}_{e0}) = (\mathbf{0}, \mathbf{0}, 0, 0)$. *Then there exists a time* $T > 0$, *and a unique solution* $(\mathbf{E}, \mathbf{B}, \mathbf{J}, \mathbf{P}, \psi) \in \left(L^\infty(0, T; (H^1(\Omega))^3) \cap H^1(0, T; (L^2(\Omega))^3)\right)^4 \times L^\infty(0, T; (H^1 \cap H_1))$ *to Equations* (1a), (1b), *and* (2b) *(with* $m = 1$*),* (5), (41), *and* (42).

In the case of the MASP model supplemented by the evolution equations (41) and (42), we first need to adjust several lemmas proven above. In particular, Lemmas 3.4 and 3.5 are still true for $\mathbf{x}' = \mathbf{x}'_1$, i.e. in the first gas "cell" only. However, inside the gas subdomain we have to consider the evolution equations, in particular

$$(43) \qquad \partial_t^2\mathbf{P} = v_g^2 \triangle\mathbf{P}.$$

LEMMA 3.13. *We assume Dirichlet BCs on* $\partial\Omega$: $\mathbf{P}(t)|_{\partial\Omega} = \mathbf{0} \in \mathbb{R}^3$, *then for all* $T > 0$, *and* $\Omega \subset \mathbb{R}^3$

$$(44) \quad \begin{aligned} &\|\partial_t\mathbf{P}(\cdot, T)\|^2_{\left(L^2(\Omega)\right)^3} + v_g^2\|\nabla \times \mathbf{P}(\cdot, T)\|^2_{\left(L^2(\Omega)\right)^3} = \|(\partial_t\mathbf{P})_0(\cdot)\|^2_{\left(L^2(\Omega)\right)^3} + \\ &+ v_g^2\|(\nabla \times \mathbf{P})_0(\cdot)\|^2_{\left(L^2(\Omega)\right)^3} + 2v_g^2\int_0^T\int_\Omega \partial_t\mathbf{P}(\mathbf{x}', t) \cdot \nabla\mathcal{N}_e(\mathbf{x}', t)d\mathbf{x}'dt. \end{aligned}$$

Proof. We multiply (43) by $\partial_t\mathbf{P}$ and consider separately the LHS and the RHS:

$$(45) \qquad \partial_t\mathbf{P} \cdot \partial_t^2\mathbf{P} = \frac{1}{2}\partial_t|\partial_t\mathbf{P}|^2,$$

$$(46) \qquad \partial_t\mathbf{P} \cdot \triangle\mathbf{P} = (\partial_t\mathbf{P} \cdot \nabla)(\nabla \cdot \mathbf{P}) - \partial_t\mathbf{P} \cdot [\nabla \times [\nabla \times \mathbf{P}]],$$

where $|\partial_t\mathbf{P}|^2 = \partial_t\mathbf{P} \cdot \partial_t\mathbf{P}$.

Recall that $\nabla \cdot \mathbf{P} = -(\mathcal{N} - \mathcal{N}_e)$, so the first term of the RHS reads
$$(\partial_t\mathbf{P} \cdot \nabla)(\nabla \cdot \mathbf{P}) = -(\partial_t\mathbf{P} \cdot \nabla)(\mathcal{N} - \mathcal{N}_e) = \partial_t\mathbf{P} \cdot \nabla\mathcal{N}_e.$$

The second term in (46) can be rewritten
$$\partial_t\mathbf{P} \cdot [\nabla \times [\nabla \times \mathbf{P}]] = \nabla \cdot [[\nabla \times \mathbf{P}] \times \partial_t\mathbf{P}] + [\nabla \times \mathbf{P}] \cdot [\nabla \times \partial_t\mathbf{P}] =$$
$$= \nabla \cdot [[\nabla \times \mathbf{P}] \times \partial_t\mathbf{P}] + \frac{1}{2}\partial_t|\nabla \times \mathbf{P}|^2,$$

so finally we come to

$$(47) \qquad \partial_t\big\{|\partial_t\mathbf{P}|^2 + v_g^2|\nabla \times \mathbf{P}|^2\big\} = 2v_g^2\partial_t\mathbf{P} \cdot \nabla\mathcal{N}_e - 2v_g^2\nabla \cdot [[\nabla \times \mathbf{P}] \times \partial_t\mathbf{P}].$$

Now we integrate (47) over $(0, T) \times \Omega$ (applying the divergence theorem and using the BCs) to obtain (44). $\square$

Similarly, in addition to Lemma 3.6 we need to consider the property of $\mathcal{N}_e$ inside the subdomain.

LEMMA 3.14. *We assume Dirichlet BCs on* $\partial\Omega$: $\mathcal{N}_e(t)|_{\partial\Omega} = 0 \in \mathbb{R}$, *then for all* $T > 0$ *and* $\Omega \subset \mathbb{R}^3$

$$(48) \quad \begin{aligned} &\|\partial_t\mathcal{N}_e(\cdot, T)\|^2_{L^2(\Omega)} + v_g^2\|\nabla\mathcal{N}_e(\cdot, T)\|^2_{L^2(\Omega)} = \\ &= \|(\partial_t\mathcal{N}_e)_0(\cdot)\|^2_{L^2(\Omega)} + v_g^2\|(\nabla\mathcal{N}_e)_0(\cdot)\|^2_{L^2(\Omega)}. \end{aligned}$$

Proof. We multiply the wave equation (42) by $\partial_t \mathcal{N}_e$ and note that

$$(49) \qquad \partial_t \mathcal{N}_e \partial_t^2 \mathcal{N}_e = \frac{1}{2} (\partial_t \mathcal{N}_e)^2$$

$$\partial_t \mathcal{N}_e \triangle \mathcal{N}_e = \nabla \cdot (\partial_t \mathcal{N}_e \nabla \mathcal{N}_e) - (\nabla \mathcal{N}_e) \cdot (\nabla \partial_t \mathcal{N}_e) =$$

$$(50) \qquad = \nabla \cdot (\partial_t \mathcal{N}_e \nabla \mathcal{N}_e) - \frac{1}{2} \partial_t (\nabla \mathcal{N}_e)^2.$$

Then we integrate both sides over $(0, T) \times \Omega$ to (48). $\qquad\qquad\qquad\square$

LEMMA 3.15. *There exists a constant $C_1 > 0$, such that for all $T > 0$*

$$(51) \qquad \sup_{0 \le t \le T} \|\mathcal{N}_e(\cdot, t)\|_{H^1(\Omega)}^2 \le C_1.$$

Proof. From $\partial_t \mathcal{N}_e^2 = 2\mathcal{N}_e \partial_t \mathcal{N}_e$ we deduce

$$\|\mathcal{N}_e(\cdot, T)\|_{L^2(\Omega)}^2 \le \|\mathcal{N}_{e0}\|_{L^2(\Omega)}^2 + \eta^{-1} \int_0^T \|\mathcal{N}_e(\cdot, T)\|_{L^2(\Omega)}^2 dt +$$

$$(52) \qquad + \eta \int_0^T \|\partial_t \mathcal{N}_e(\cdot, T)\|_{L^2(\Omega)}^2 dt.$$

From now on in current section, η is defined in the same way as in Remark 3.10. Then from (48) and (52) and Grönwall's inequality we come to (51). $\qquad\square$

LEMMA 3.16. *There exists a constant $C_2 > 0$ such that for all $T > 0$*

$$(53) \qquad \sup_{0 \le t \le T} \|\mathbf{P}(\cdot, t)\|_{(H^1(\Omega))^3}^2 \le C_2.$$

Proof. From Lemma 3.13 and for all $t > 0$

$$\|\partial_t \mathbf{P}(\cdot, T)\|_{\left(L^2(\Omega)\right)^3}^2 + v_g^2 \|\nabla \times \mathbf{P}(\cdot, T)\|_{\left(L^2(\Omega)\right)^3}^2 \le \|(\partial_t \mathbf{P})_0\|_{\left(L^2(\Omega)\right)^3}^2 +$$

$$(54) \qquad + v_g^2 \|(\nabla \times \mathbf{P})_0\|_{\left(L^2(\Omega)\right)^3}^2 + \eta^{-1} \int_0^T \|\partial_t \mathbf{P}(\cdot, t)\|_{\left(L^2(\Omega)\right)^3}^2 dt +$$

$$+ \eta v_g^4 \int_0^T \|\nabla \mathcal{N}_e(\cdot, t)\|_{L^2(\Omega)}^2 dt.$$

Thus, we can conclude by Grönwall's inequality and (51) that $\|\partial_t \mathbf{P}(\cdot, T)\|_{\left(L^2(\Omega)\right)^3}^2$ and $\|\nabla \times \mathbf{P}(\cdot, T)\|_{\left(L^2(\Omega)\right)^3}^2$ are bounded. We recall that according Lemma 3.15 and relation $\nabla \cdot \mathbf{P} = -(\mathcal{N} - \mathcal{N}_e)$, norm $\|\nabla \cdot \mathbf{P}(\cdot, T)\|_{L^2(\Omega)}^2$ is bounded as well. Hence from $\partial_t \mathbf{P}^2 = \mathbf{P} \partial_t \mathbf{P}$ we obtain

$$\|\mathbf{P}(\cdot, T)\|_{\left(L^2(\Omega)\right)^3}^2 \le \|\mathbf{P}_0\|_{\left(L^2(\Omega)\right)^3}^2 +$$

$$+ \eta^{-1} \int_0^T \|\mathbf{P}(\cdot, t)\|_{\left(L^2(\Omega)\right)^3}^2 dt + \eta \int_0^T \|\partial_t \mathbf{P}(\cdot, t)\|_{\left(L^2(\Omega)\right)^3}^2 dt,$$

thus, again with Grönwall's inequality and (54) we deduce (53). $\qquad\square$

Note that from Lemma 3.15 we deduce boundedness of $\|\partial_t (\nabla \cdot \mathbf{P})(\cdot, T)\|_{L^2(\Omega)}^2 = \|\partial_t \mathcal{N}_e(\cdot, T)\|_{L^2(\Omega)}^2$ and then deduce (53). That means, all needed conditions to prove Lemma 3.11 are satisfied. Now we can extend Lemma 3.11 in the case of the enriched MASP model.

LEMMA 3.17. *There exists a constant $C > 0$ such that for all $T > 0$*

$$
\begin{aligned}
(55) \quad &\sup_{0 \leq t \leq T} \|\mathbf{E}(\cdot, t)\|^2_{(H^1(\Omega))^3} + \sup_{0 \leq t \leq T} \|\mathbf{B}(\cdot, t)\|^2_{(H^1(\Omega))^3} + \\
&+ \eta^2 \sup_{0 \leq t \leq T} \|\mathbf{J}(\cdot, t)\|^2_{(H^1(\Omega))^3} + \sup_{0 \leq t \leq T} \|\mathbf{P}(\cdot, t)\|^2_{(H^1(\Omega))^3} \leq C.
\end{aligned}
$$

Proof. We can deduce this result from Lemma 3.11 and Lemma 3.16. ∎

Proof. of Theorem 3.12. As in the proof of Theorem 3.1, the existence is based on Leray-Schauder's fixed point theorem [33]. In Lemmas 3.2 to 3.9 and 3.11 and Lemmas 3.13 to 3.16, we proved that for all $T > 0$ there exists a constant $C > 0$ such that:

$$
\begin{aligned}
&\|\mathbf{E}\|^2_{L^\infty\left(0,T;(H^1(\Omega))^3\right) \cap H^1\left(0,T;(L^2(\Omega))^3\right)} + \|\mathbf{B}\|^2_{L^\infty\left(0,T;(H^1(\Omega))^3\right) \cap H^1\left(0,T;(L^2(\Omega))^3\right)} + \\
&+ \eta^2 \|\mathbf{J}\|^2_{L^\infty\left(0,T;(H^1(\Omega))^3\right) \cap H^1\left(0,T;(L^2(\Omega))^3\right)} + \|\mathbf{P}\|^2_{L^\infty\left(0,T;(H^1(\Omega))^3\right) \cap H^1\left(0,T;(L^2(\Omega))^3\right)} + \\
&+ \mu\|\psi\|_{L^\infty\left(0,T;(H^1 \cap H_1)\right)} \leq C,
\end{aligned}
$$

and $L^\infty\left(0, T; (H^1(\Omega))^3\right) \times L^\infty\left(0, T; (H^1 \cap H_1)\right)$ is compactly embedded in $L^2(\Omega \times (0, T]) \times (L^2(\mathbb{R}^3 \times \mathbb{R}_+))$. The approach follows [49]. We introduce a continuous mapping derived from (1a), (1b), (2b), (5), (41), and (42), that depends on a parameter $\lambda \in [0, 1]$ and that admits a fixed point in $L^2(\Omega \times (0, T]) \times (L^2(\mathbb{R}^3 \times \mathbb{R}_+))$ as verifying Leray-Schauder's theorem assumptions.

To prove uniqueness, we take the difference vector $(\mathbf{E}, \mathbf{B}, \mathbf{J}, \mathbf{P}, \overline{\psi})^T := (\mathbf{E}_2 - \mathbf{E}_1, \mathbf{B}_2 - \mathbf{B}_1, \mathbf{J}_2 - \mathbf{J}_1, \mathbf{P}_2 - \mathbf{P}_1, \overline{\psi}_2 - \overline{\psi}_1)^T$, with zero ICs, where $(\mathbf{E}_1, \mathbf{B}_1, \mathbf{J}_1, \mathbf{P}_1, \overline{\psi}_1)^T$ and $(\mathbf{E}_2, \mathbf{B}_2, \mathbf{J}_2, \mathbf{P}_2, \overline{\psi}_2)^T$ denote two solutions. Then applying the methods presented in the above lemmas, see also [28], we come to the inequality with some constant $C > 0$:

$$
\begin{aligned}
(56) \quad &\frac{d}{dt}\Big\{\mu\|\overline{\psi}(t)\|^2_{(H^1 \cap H_1)} + \int_\Omega \big(\|\mathbf{E}(\mathbf{x}', t)\|^2_{\left(L^2(\Omega)\right)^3} + \|\mathbf{B}(\mathbf{x}', t)\|^2_{\left(L^2(\Omega)\right)^3} \\
&\qquad + \eta^2\|\mathbf{J}(\mathbf{x}', t)\|^2_{\left(L^2(\Omega)\right)^3} + \|\mathbf{P}(\mathbf{x}', t)\|^2_{\left(L^2(\Omega)\right)^3}\big)d\mathbf{x}'\Big\} \leq \\
&C\Big\{\mu\|\overline{\psi}(t)\|^2_{(H^1 \cap H_1)} + \int_\Omega \big(\|\mathbf{E}(\mathbf{x}', t)\|^2_{\left(L^2(\Omega)\right)^3} + \|\mathbf{B}(\mathbf{x}', t)\|^2_{\left(L^2(\Omega)\right)^3} + \\
&\qquad + \eta^2\|\mathbf{J}(\mathbf{x}', t)\|^2_{\left(L^2(\Omega)\right)^3} + \|\mathbf{P}(\mathbf{x}', t)\|^2_{\left(L^2(\Omega)\right)^3}\big)d\mathbf{x}'\Big\}.
\end{aligned}
$$

We conclude by Grönwall's inequality that $\left(\mathbf{E}(\cdot, t), \mathbf{B}(\cdot, t), \mathbf{J}(\cdot, t), \mathbf{P}(\cdot, t), \overline{\psi}(\cdot, t)\right)^T \equiv (\mathbf{0}, \mathbf{0}, \mathbf{0}, \mathbf{0})^T$ for all $t > 0$. ∎

Summarizing the outcomes of this part, because of the regularity of the solutions not only of the "pure" MASP model, but the "extended" MASP model as well.

4. Numerical Methods and Parallel Computing. For 1d Maxwells equations we use the second order Lax-Wendroff scheme, see e.g. [46], which is stable under the Courant-Fredrichs-Lewy (CFL)-condition. We solve the 2d Schrödinger equation in 3 stages using the symmetric Strang splitting of second order [44]. At the second stage, we solve the equation with static Coulomb potential using Crank-Nicolson's scheme, which is unconditionally stable. Note that we deal with the multiscale problem, where the time step Δt_S for Schrödinger's equation is much smaller than for Maxwell's equations Δt_M: $\Delta t_M / \Delta t_S = 10 \dots 20$, see also [32]. Finally, to preserve

the second order of convergence of the overall scheme, we use Adams-Bashforth's second order consistent method to solve Drude's equation (5) and Lax-Wendroff-type scheme for solving the evolution equation for polarization in its simplest (8) or nonlinear (22) form.

Now we discuss the coupling of the schemes approximating (i) the MASP model, (ii) the polarization evolution equation (15), and (iii) the free electron density evolution equation (17). As an example, we assume that the gas region L, is divided in 4 subdomains each containing N_2 Maxwell's cells, see Figure 2. At time t^n each of 4 processors solves the TDSE only in the first cell of the subdomain assigned to it, i.e. at nodes $z'_{\alpha,1}$, where $\alpha = \{1, 2, 3, 4\}$ is the ordinal number of the subdomain, and the second index corresponds to the position number within the subdomain, see Figure 3. Then the data $(\partial_t \mathbf{P})^n_{\alpha,1}$ and $(\mathcal{N}_e)^n_{\alpha,1}$ are sent to the root processor in order to update (i) the current of free electrons $\mathbf{J}^{n*}_{\alpha,\mu}$, and then (ii) the EM field at time t^{n**}: $\mathbf{E}^{n**}_{\alpha,\mu}$, $\mathbf{B}^{n**}_{\alpha,\mu}$, $\mu = 1, \ldots, N_2$. Note that at this point, we assume that the root processor knows the values of $(\partial_t \mathbf{P})^n_{\alpha,\mu}$ and $(\mathcal{N}_e)^n_{\alpha,\mu}$ for *all* spatial points $z'_{\alpha,\mu}$ ($\alpha = 1, \ldots, 4$, $\mu = 1, \ldots, N_2$), but not only for the first cells $\{z'_{\alpha,1}\}$ where the TDSEs are solved. To clarify that apparent contradiction, we point out that at the time $t \in (t^{n**}, t^{n+1})$, the root processor evaluates $(\partial_t \mathbf{P})^{n+1}_{\alpha,\mu}$ and $(\mathcal{N}_e)^{n+1}_{\alpha,\mu}$ for the *next* time cycle, in all Maxwell's cells using the evolution equations for the polarization and the free electron density. Finally, we generalize the described scheme in the case of m subdomains and l processors, requiring the ratio m/l to be an integer.

5. Numerical Experiments. In this section, we present some results obtained with the enriched MASP model, and compare them with those obtained with the "pure" MASP model.
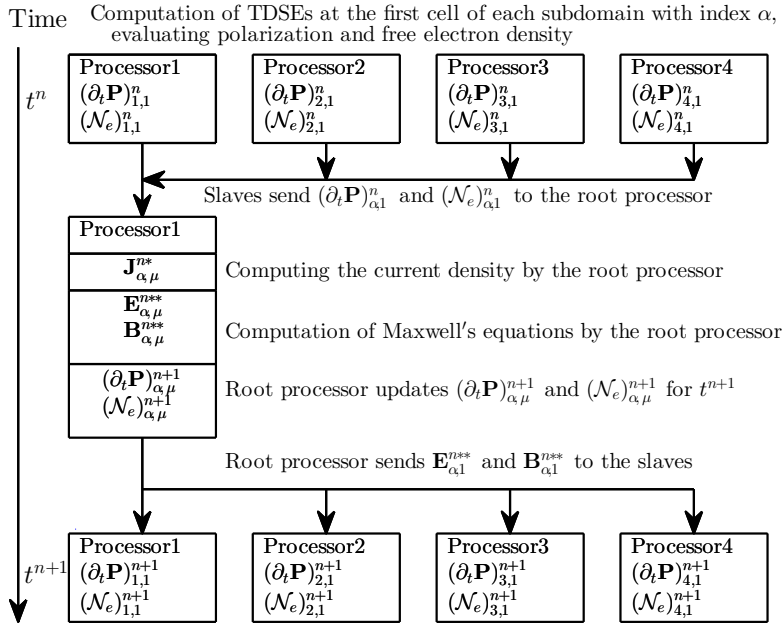
FIG. 3. *Example of parallelization: 1d-2d MASP model enriched by the evolution equations. Index of subdomain $\alpha = 1 \ldots N_1$ (here $N_1 = 4$), index of the cell in the subdomain $\mu = 1 \ldots N_2$. Length of the gas region $L = 4 \times N_2 \times \Delta z'$.*

5.1. The MASP Model Enriched by the Simple Evolution Equation.
We start by reporting the results of the 1d-2d MS model supplemented by the homogeneous transport equation (8), setting first $v_g = c$. The propagation path of the pulse in the gas region L, is divided into N_1 subdomains, each containing N_2 Maxwell's cells, see Figure 2. At each Maxwell's time step, the TDSEs are solved several times (as $\Delta t_M / \Delta t_S \geq 10$) to provide the values of **P** in the first cells of each subdomain. The polarization in the remaining cells of the subdomains is supposed to be computed from the macroscopic transport equation (8) at the previous time step. The corresponding parallel computing strategy is presented in Figure 3.

We present in Figure 4, the spectral intensity $I(\omega)$ of the linearly polarized pulse, whose field vector **E** is parallel to the axis of H_2^+-molecule. The spectral intensity is computed via the Fourier transform of the electric field: $I(\omega) = c|\widehat{\mathbf{E}}(\omega)|^2/8\pi$, as soon as the pulse envelope escapes from the gas region and appears "as a whole" in the last vacuum region. As we see, when the initial intensity is not high, e.g. $I = 5 \times 10^{13}$ W/cm^2, the MS model enriched even by the simplest evolution equation provides decent approximations of spectra depending on the chosen partitions of the total number of cells in the gas region N into number of subdomains N_1 and number of cells per each subdomain N_2 (see the legend).

Within the same approach we also modeled the propagation of the circularly polarized initial pulse. In particular, we report in Figure 5 the intensities of the first generated odd harmonics as functions of the propagation length in the gas. Compar-
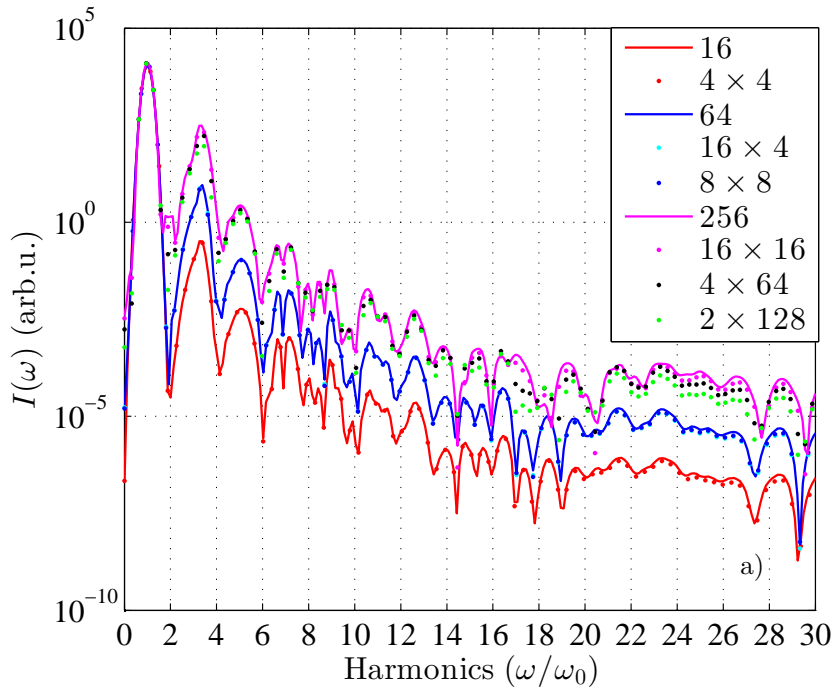
FIG. 4. *Spectral intensities of the electric field harmonics for different gas region lengths; $\lambda = 800$ nm, $I = 5 \times 10^{13}$ W/cm^2, $\Delta z_M = 100$ a.u., so that $L = 100 \times N$ a.u. (see the legend for values of $N = N_1 \times N_2$). The grid for solving 2-d TDSE is 300×300 with step $\Delta x_S = \Delta y_S = 0.3$ a.u., gas density $\mathcal{N} = 5.17 \times 10^{-5}$ a.u.*
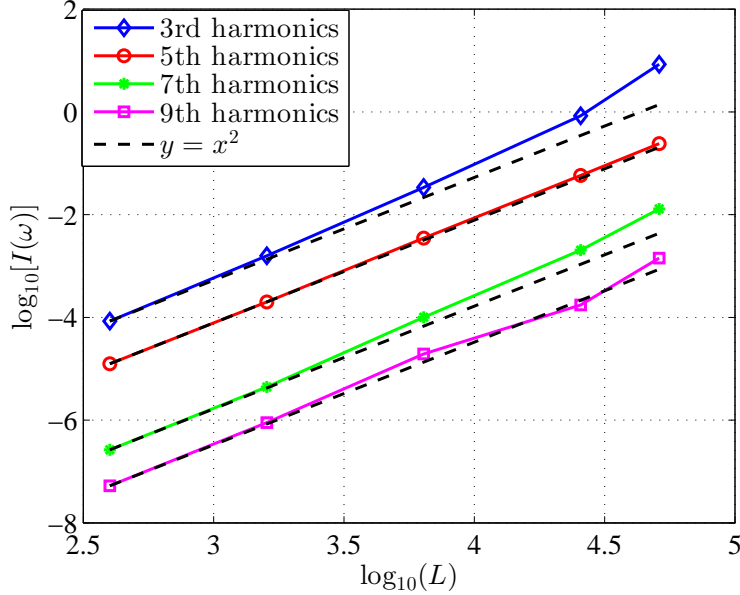
Fig. 5. *Intensity of the low order harmonics of the circularly polarized pulse as a function of the propagation length in a gas:* $L = 100 \times N$ ($N = 4, 16, 64, 16 \times 16$ and 32×16) *a.u.;* $\lambda = 800$ *nm,* $I = 5 \times 10^{13}$ W/cm^2. *The grid for solving 2-d TDSE is* 500×500 *with step* $\Delta x_S = \Delta y_S = 0.3$ *a.u., gas density* $\mathcal{N} = 5.17 \times 10^{-5}$ *a.u.*

ing this graph with results from [32], computed within the "pure" model, we observe the concordance of the results within 5%, even though the new data were obtained at a much lower cost of computing effort. Indeed, the suggested approach helps to reduce the computational complexity with respect to the original model. Table 1 shows that the processing times for the cases of the "pure" Maxwell-Schrödinger model and the MS model enriched by the polarization evolution equation are comparable, while in the first case the number of the engaged processors is up to 16-fold. For example, in the case of circularly polarized initial pulse, the same spectrum was obtained for the same times but using 256 processors ("pure" model) and 16 processors (MS model coupling with the polarization evolution equation). Note that the computational times for the circularly polarized-case are higher, as we here used 500×500 points grids to solve the TDSE, while in LP-case 300×300 points grids are sufficient to properly computes of the wavefunctions.

TABLE 1

Processing times for computation of propagation of linearly polarized (LP) and circularly polarized (CP) pulses in the gas, depending on the product of the number of subdomains (N_1) and the number of cells per subdomain (N_2)

$N_1 \times N_2$	64	8×8	256	16×16
Proc. time (LP) (h:m)	03:49	03:56	04:35	04:44
Proc. time (CP) (h:m)	–	–	13:35	13:04

5.2. The MASP Model Enriched by the Nonlinear Evolution Equation. In order to simulate the propagation of pulses with higher initial intensities, we consider the more complicated polarization evolution equation (22). Further, we will compare the transmitted electric fields and spectra computed using the models enriched by the nonlinear and simple polarization equations with the results of the "pure" MS/MASP models, considering the latter as reference data, see Figure 6. Let us briefly discuss these figures. Note that in our computations we used different intensities of the initial pulse, $I_1 = 10^{14}$ W/cm^2, $I_2 = 5 \times 10^{14}$ W/cm^2 and different number densities $\mathcal{N}_{01} = 1.63 \times 10^{-5}$ a.u. and $\mathcal{N}_{02} = 5.17 \times 10^{-5}$ a.u. It is clear that the higher intensity of the pulse and density of the gas, the greater influence of the free electron currents on dynamics of the process. For example, in case of initial pulse with I_1, L^2-norm of the wavefunction is $\|\psi\|^2_{L^2} \approx 0.66$, while in case of I_2 we obtained $\|\psi\|^2_{L^2} \approx 10^{-6}$, which results in significant difference in the free electron number density (18). That is why the computations involving I_2 were performed with the MASP model. Recall that unlike the MS model, the MASP model takes into account the currents of free electrons.

(a)

(b)
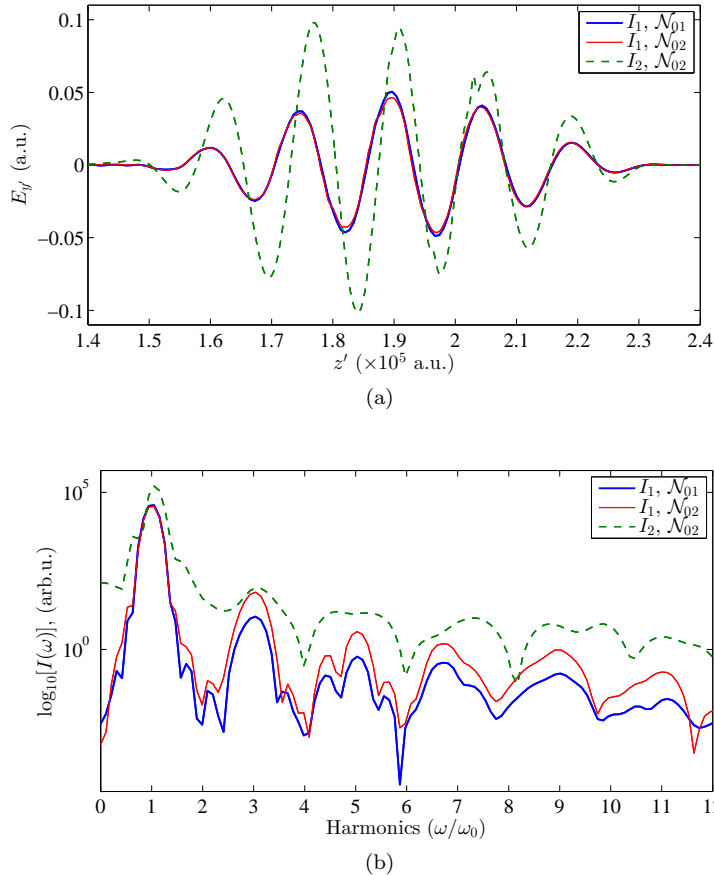
FIG. 6. *Results of the pure MASP model: a) electric field as a function of space and b) spectral intensity of the laser pulse after propagation through the gas region $L = 4 \times 64 \times 100$ a.u. Initial pulse intensities: $I_1 = 10^{14}$ W/cm^2, $I_2 = 5 \times 10^{14}$ W/cm^2, number density of thee gas: $\mathcal{N}_{01} = 1.63 \times 10^{-5}$ a.u., $\mathcal{N}_{02} = 5.17 \times 10^{-5}$ a.u.*

As we see from Figures 6a and 6b, if we consider pulses with the same initial intensity I_1, but propagating in gases of different density, for definiteness $\mathcal{N}_{01} < \mathcal{N}_{02}$, the amplitude of the transmitted electric field is a bit lower in the case of a higher density, due to stronger ionization losses. However, the generation of the high odd harmonics is more intense for $\mathcal{N}_{02}$, see Figure 6b, as the polarization of the medium is proportional to the gas number density. On the other hand, in the case of initial intensity $I_2 > I_1$ the level of ionization becomes much higher (with respect to initial intensity I_1). As a result, the amplitudes of the high harmonics are relatively smaller.

Including the instantaneous susceptibility coefficient $\chi^{(3)}$ (or even $\chi^{(5)}$, $\chi^{(7)}$ and so on) as a parameter in the polarization evolution equation (22), we are pursuing two objectives: to describe more accurately (i) the electromagnetic field profile, and (ii) the spectrum of harmonics. In the following set of figures, we report the data computed within the MASP model supplemented by the evolution equations. We start from the length of the gas region $L = 256 \times 100$ a.u., with propagation time $T = 1051.87$ a.u. We use 3 different values of $\chi^{(3)}$ to test the model. At first glance, even simulations engaging the transport equation with $v_g = c$ and $\chi^{(3)} = 0$, describe the field profile decently; however, as we are comparing the corrections for nonlinear effects accumulating very slowly, we need to pay attention to the very top parts of the electric field profiles, see Figure 7. Then we notice with initial intensity I_1, the parameter $\chi^{(3)} = 10^{-4}$ works better for both gas densities. In Figure 8, we also report ℓ_2 and ℓ_∞-norms of the solutions presented in Figure 7b and the errors computed with respect to the "pure" MASP model. As we observe, in all the figures the dashed blue curves corresponding to $\chi^{(3)} = 10^{-4}$ provides the closest agreement with the results of the "pure" MASP model in conformity with results in Figure 7.

Now we proceed to the presentation of the high harmonics spectra, see Figure 9. The simulation parameters for these spectra are exactly the same as for Figure 7. We observe that the selection $\chi^{(3)} = 4 \times 10^{-4}$ a.u. yields less precise results than the two other options. In this case, we are overestimating again the response of the bound electrons. Moreover, the evolution equation (22) with $\chi^{(3)}$ in the RHS, may account corrections to polarization of the 3rd harmonic only, while these computations seems to be adequate even with homogeneous transport equation (8).

The situation changes at higher initial intensities, e.g. $I_2 = 5 \times 10^{14}$ W/cm^2 that, as we know, results in significant ionization. In this case, introducing instantaneous nonlinear susceptibility does not seem appropriate. In Figure 10a, we observe the differences between the solutions of the "pure" and "enriched" MASP models. This was expected, as $\chi^{(3)}$ describes the response of bound electrons, whose number is way below the number of free electrons at high intensity. Even so, we still can rely on simulation with the transport equation as it follows from comparison between the heavy black and the thin red curves in Figure 10a.

In Figure 10b we report the high harmonic spectra formed after propagation of the pulse of initial intensity $I_2 = 5 \times 10^{14}$ W/cm^2 through the gas. The first three solutions (according to the legend) correspond to the electric field profiles represented in Figure 10. The 4th solution was obtained under the assumption $\mathbf{J} = 0$, which as we know is wrong for that intensity. In the large, one can observe the best convergence, inter alia, between solutions of the pure MASP model (heavy black curves on Figures 10a and 10b) and those of the MASP model enriched by the homogeneous transport equation (thin red curves). Just as expected (see the dashed blue curve), adding the perturbative term with $\chi^{(3)}$ to the polarization equation is unsuitable in such ionized gas. We also deduce that including the free electron currents in the model is essential, as the solution in magenta, see Figure 10b, is not a good candidate to fit

(a)

(b)
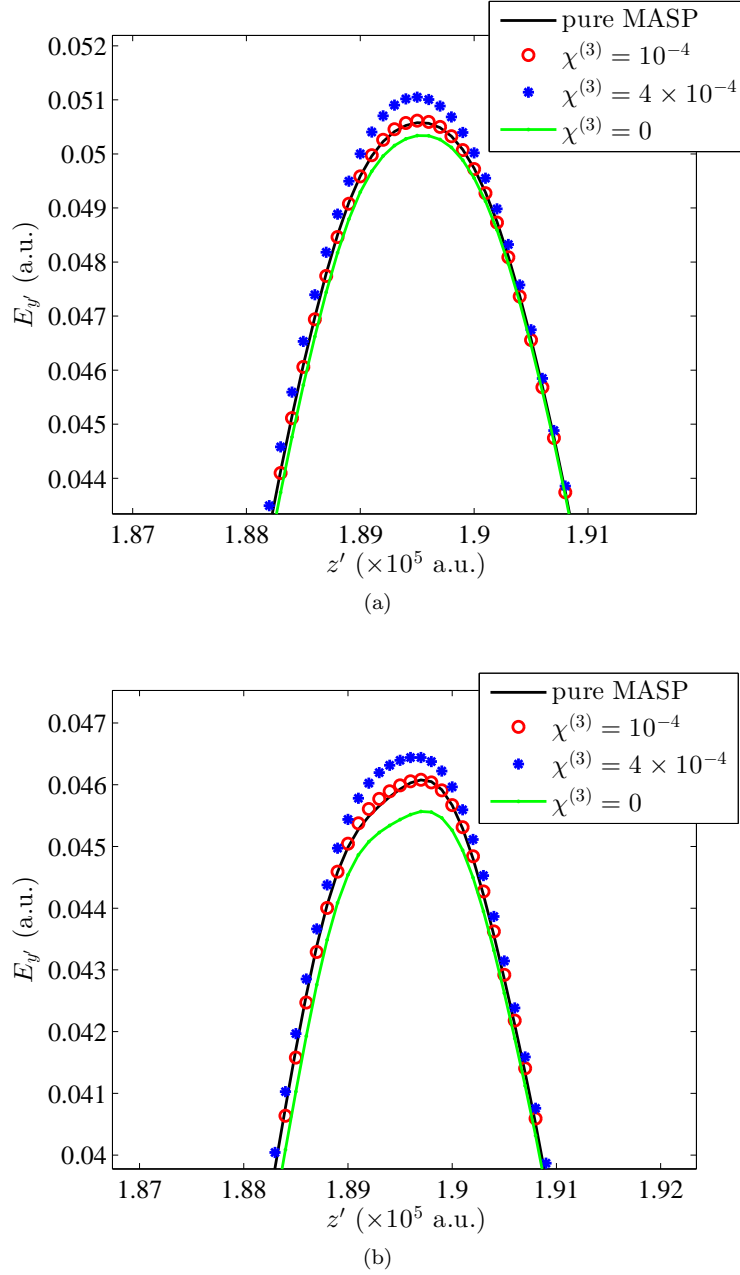
FIG. 7. *Results of the MASP model supplemented by the polarization evolution equation in comparison with the results of the "pure" MASP model: transmitted electric fields for initial intensity $I_1 = 10^{14}$ W/cm^2 and gas number density a) $\mathcal{N}_{01} = 1.63 \times 10^{-5}$ a.u., b) $\mathcal{N}_{02} = 5.17 \times 10^{-5}$ a.u. Propagation length in gas $L = 256 \times 100$ a.u., which in case of engaging the evolution equation is divided into 4 subdomains each containing 64 cells. Linear instantaneous susceptibility for polarization equation $\chi^{(1)} = 1.83 \times 10^{-5}$, while the coefficient $\chi^{(3)}$ is a model parameter, see the legends.*

the "pure" MASP model solution.

Regarding the accurate simulations of the high harmonics spectra within the enriched model, the most important factor (than nonlinearity in the polarization equation) is how Maxwell's domain is decomposed in subdomains, see Figures 11a and 11b where the propagation length is $L = 204800$ a.u. Say, decomposition into 32 subdomains each containing 64 cells, allows us to simulate accurately up to 35 harmonics, while spending less computing resources: 94 h×256 proc vs. 12 h×32 proc. Moreover, if we are interested in the first 11 harmonics only, we can use decomposition 8×256, which takes 12 h×8 proc.
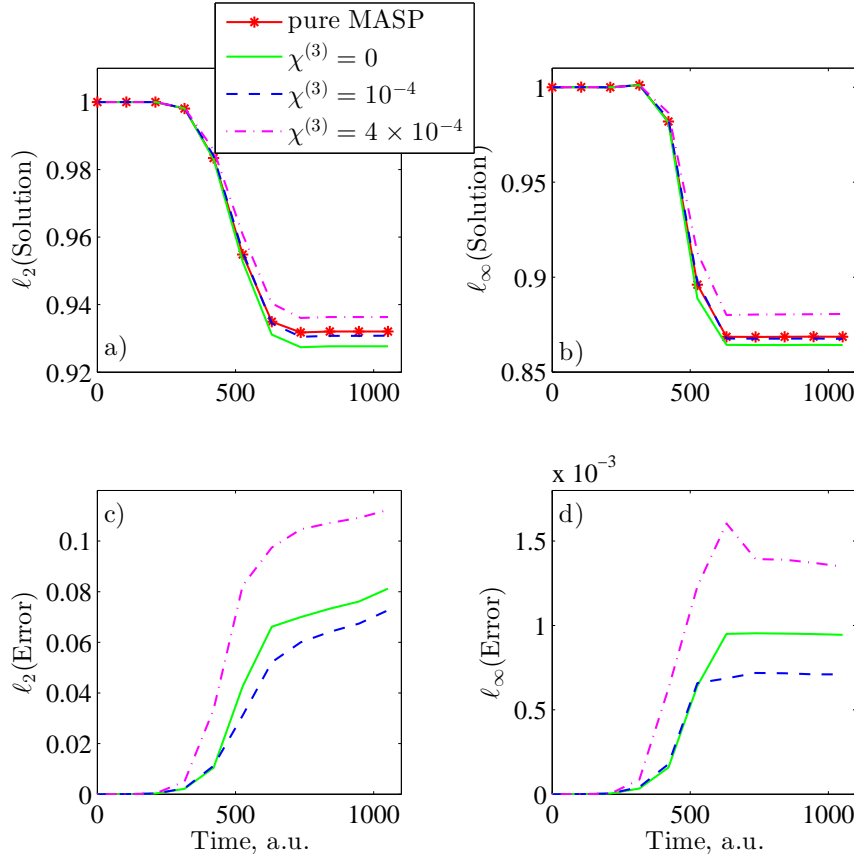
FIG. 8. *a) ℓ_2-norms of solutions presented in Figure 7b; b) ℓ_∞-norms of the same solutions; c) ℓ_2-norms of errors of these solutions with respect to the MASP model results; d) ℓ_∞-norms of errors of these solutions with respect to the MASP model results.*
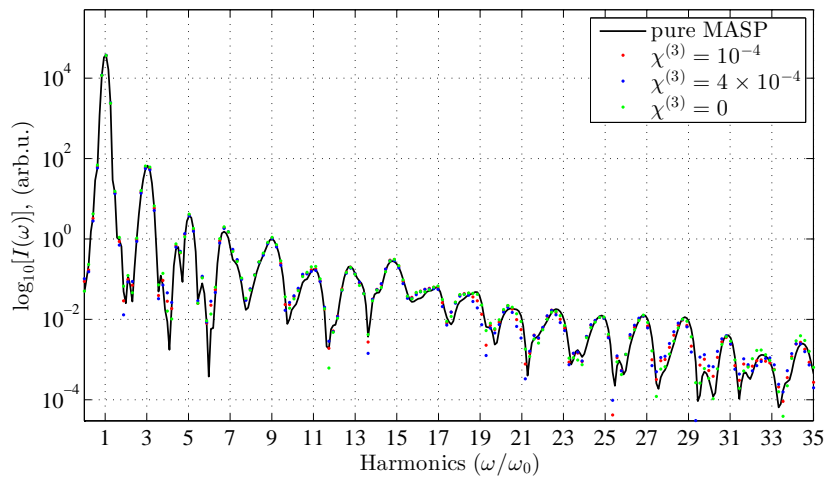
(a)
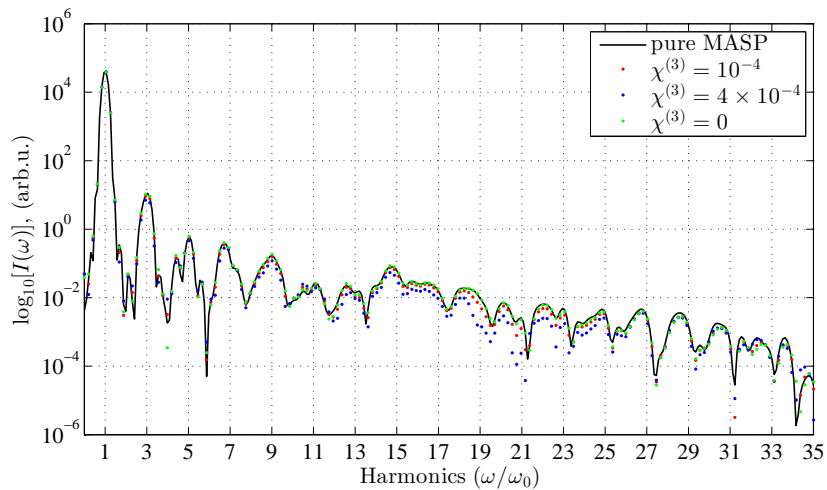
(b)

FIG. 9. *Spectral intensities of high harmonics. The same parameters as for Figures 7a and 7b.*

(a)

(b)
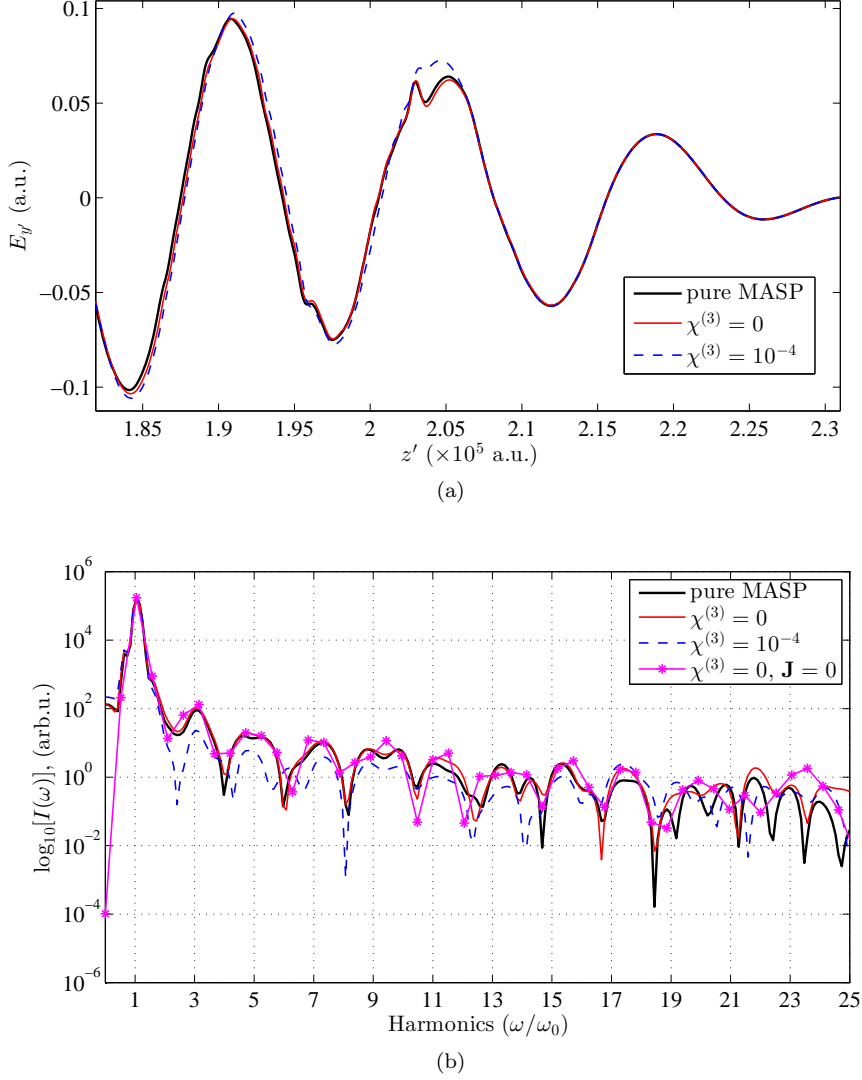
FIG. 10. *Results of the MASP model supplemented by the polarization evolution equation in comparison with the results of the "pure" MASP model: (a) transmitted electric fields for initial intensity $I_2 = 5 \times 10^{14}$ W/cm^2 and gas number density $\mathcal{N}_{02} = 5.17 \times 10^{-5}$ a.u. Path in a gas $L = 256 \times 100$ a.u., divided into 4 subdomains each containing 64 cells, $\chi^{(1)} = 1.83 \times 10^{-5}$, $\chi^{(3)}$ is a model parameter, see the legends; (b) Spectral Intensity for solutions shown in panel (a), additional solution computed in case $\mathbf{J} = 0$.*

(a)

(b)
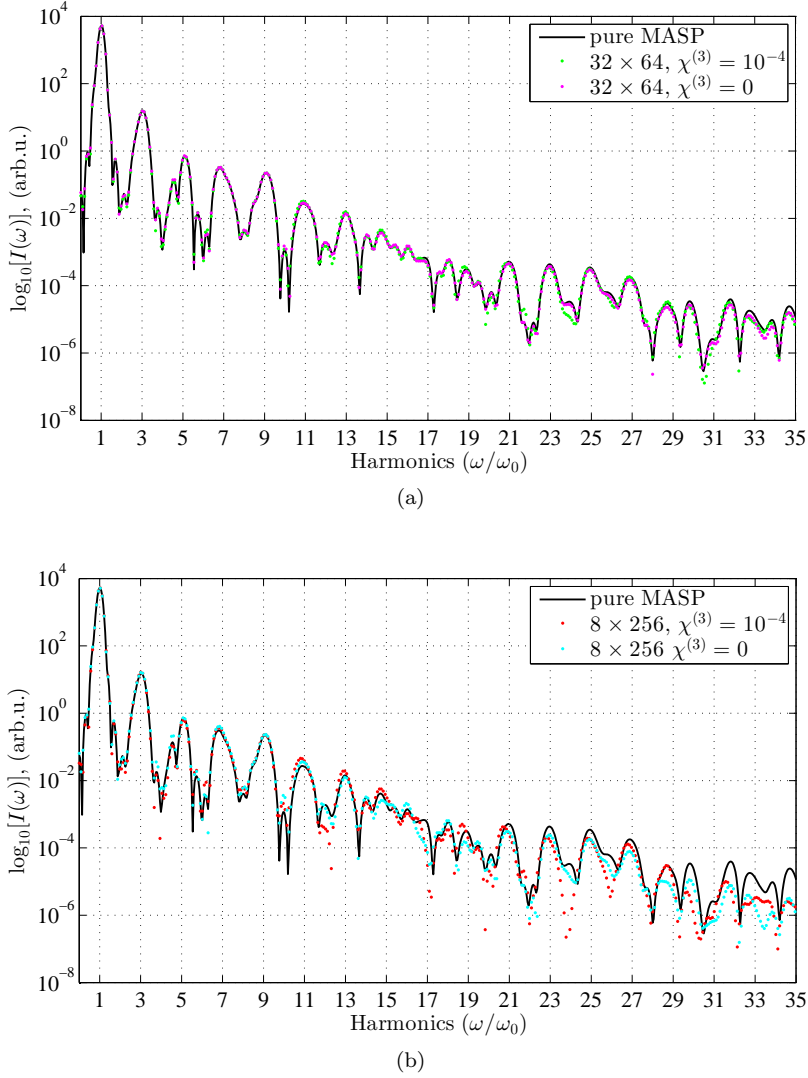
FIG. 11. *Spectra of high harmonics obtained within the "pure" MASP model and using the evolution equation for polarization. The pulse initial intensity $I_1 = 10^{14}$ W/cm^2, gas density $\mathcal{N}_{01} = 1.63 \times 10^{-5}$ a.u., propagation length in a gas $L = 204800$ a.u. (0.01 mm), which is divided into a) 32 subdomains each containing 64 cells and b) 8 sundomains each containing 256 cells.*

6. Conclusion. We have derived and studied some extensions of the MASP model [28, 29], allowing for a wider range of application of this generic nonperturbative model. We have demonstrated that including a polarization evolution equation to the MASP model allows for a significant reduction of the overall computational cost of the original model. We found out that the most universal type of this equation is the homogeneous transport equation. More complex nonlinear polarization equations can be useful when the level of ionization is moderate. By contrast, at high intensity (resulting in high level of ionization), the cheapest choice is the homogeneous transport equation, especially for simulating high order harmonic spectra. In this case, it is shown that the current of free electrons must also be included in the model.

REFERENCES

[1] M. Ammosov, N. Delone, and V. Krainov, *Tunnel ionization of complex atoms and atomic ions in electromagnetic field*, Sov. Phys. JETP, 91 (1986), pp. 2008–2013.

[2] I. Babushkin and L. Bergé, *The fundamental solution of the unidirectional pulse propagation equation*, J. Math. Phys., 55 (2014), 032903.

[3] A. Bandrauk, E. Lorin, and J. Moloney, eds., *Laser Filamentation. Mathematical Methods and Models.*, CRM Series in Mathematical Physics, Springer, 2016.

[4] L. Baudouin, O. Kavan, and J.-P. Puel, *Regularity for a Schrödinger equation with singular potential and application to bilinear optimal control*, J. Differential Equations, 216 (2005), pp. 188–222.

[5] P. Béjot, E. Cormier, E. Hertz, B. Lavorel, J. Kasparian, J.-P. Wolf, and O. Faucher, *High-field quantum calculation reveals time-dependent negative kerr contribution*, Phys. Rev. Lett., 110 (2013), 043902.

[6] P. Béjot, J. Kasparian, S. Henin, V. Loriot, T. Vieillard, E. Hertz, O. Faucher, B. Lavorel, and J.-P. Wolf, *Higher-order Kerr terms allow ionization-free filamentation in gases*, Phys. Rev. Lett., 104 (2010), 103903.

[7] L. Bergé, C. Gouédard, J. Schjodt-Eriksen, and H. Ward, *Filamentation patterns in Kerr media vs. beam shape robustness, nonlinear saturation and polarization states*, Phys. D, 176 (2003), pp. 181–211.

[8] L. Bergé, S. Skupin, R. Nuter, J. Kasparian, and J.-P. Wolf, *Ultrashort filaments of light in weakly ionized, optically transparent media*, Rep. Progr. Phys., 70 (2007), pp. 1633–1713.

[9] R. W. Boyd, *Nonlinear Optics*, Academic Press, 3rd ed., 2008.

[10] T. Brabec and F. Krausz, *Nonlinear optical pulse propagation in the single-cycle regime*, Phys. Rev. Lett., 78 (1997), pp. 3282–3285.

[11] T. Brabec and F. Krausz, *Intense few-cycle laser fields: Frontiers of nonlinear optics*, Rev. Modern Phys., 72 (2000), pp. 545–591.

[12] A. Braun, G. Korn, X. Liu, D. Du, J. Squier, and G. Mourou, *Self-channeling of high-peak-power femtosecond laser pulses in air.*, Opt. Lett., 20 (1995), pp. 73–75.

[13] S. Champeaux, L. Bergé, D. Gordon, A. Ting, J. Peano, and P. Sprangle, *(3+1) -dimensional numerical simulations of femtosecond laser filaments in air: Toward a quantitative agreement with experiments*, Phys. Rev. E, 77 (2008), 036406.

[14] S. Chelkowski, C. Foisy, and A. Bandrauk, *Electron-nuclear dynamics of multiphoton H_2^+ dissociative ionization in intense laser field*, Phys. Rev. A, 57 (1998), pp. 1176–1185.

[15] F. Chen, *Introduction to plasma physics and controlled fusion. V.1: Plasma Physics.*, Plenum Press. New York, 2nd ed., 1984.

[16] A. Couairon and A. Mysyrowicz, *Organizing multiple femtosecond filaments in air*, Phys. Rep., 41 (2007), pp. 47–189.

[17] M. Ferray, A. L'Huillier, X. F. Li, L. A. Lompre, G. Mainfray, and C. Manus, *Multiple-harmonic conversion of 1064 nm radiation in rare gases*, J. Phys. B, 21 (1988), pp. L31–L35.

[18] J.-Y. Ge and Z. Zhang, *Use of negative complex potential as absorbing potential*, J. Chem. Phys., 108 (1998), pp. 1429–1432.

[19] A. Husakou and J. Herrmann, *Supercontinuum generation of higher-order solitons by fission in photonic crystal fibers*, Phys. Rev. Lett., 87 (2001), 203901.

[20] R. Iório Jr. and D. Marchesin, *On the Schrödinger equation with time-dependent electric fields*, Proc. Roy. Soc. Edinburgh Sect. A, 96 (1984), pp. 117–134.

[21] V. Kalosha and J. Herrmann, *Self-phase modulation and compression of few-optical-cycle pulses.*, Phys. Rev. A, 62 (2000), p. 011804(R).

[22] L. Keldysh, *Ionization in field of a strong electromagnetic wave*, Sov. Phys. JETP, 20 (1965), pp. 1307–1314.

[23] C. Köhler, R. Guichard, E. Lorin, S. Chelkowski, A. Bandrauk, L. Bergé, and S. Skupin, *Saturation of the nonlinear refractive index in atomic gases*, Phys. Rev. A, 87 (2013), 043811.

[24] M. Kolesik and J. Moloney, *Nonlinear optical pulse propagation simulation: From Maxwell's to unidirectional equations*, Phys. Rev. E, 70 (2004), 036604.

[25] M. Kolesik and J. Moloney, *Modeling and simulation techniques in extreme nonlinear optics of gaseous and condensed media*, Rep. Progr. Phys., 77 (2014), 016401.

[26] M. Kolesik, E. M. Wright, and J. V. Moloney, *Femtosecond filamentation in air and higher-order nonlinearities*, Opt. Lett., 35 (2010), pp. 2550–2552.

[27] E. Lorin, S. Chelkowski, and A. Bandrauk, *A numerical Maxwell-Schrödinger model for laser-matter interaction and propagation*, Comput. Phys. Commun., 177 (2007), pp. 908–932.

[28] E. Lorin, S. Chelkowski, and A. Bandrauk, *The WASP model: A micro-macro system of wave-Schrödinger-plasma equations for filamentation*, Commun. Comput. Phys., 9 (2011), pp. 406–440.

[29] E. Lorin, S. Chelkowski, E. Zaoui, and A. Bandrauk, *Maxwell-Schroedinger-Plasma (MASP) model for laser-molecule interactions: towards quantum filamentation with intense ultrashort pulses*, Phys. D, 241 (2012), pp. 1059–1071.

[30] E. Lorin, M. Lytova, and A. Bandrauk, in Laser Filamentation. Mathematical Methods and Models, A.Bandrauk, E.Lorin and J.Moloney, eds., (2016), pp. 167–183.

[31] E. Lorin, M. Lytova, A. Memarian, and A. Bandrauk, *Development of nonperturbative nonlinear optics models including effects of high order nonlinearities and of free electron plasma: Maxwell-Schrödinger equations coupled with evolution equations for polarization effects, and the sfa-like nonlinear optics model*, J. Phys. A, 48 (2015), 105201.

[32] M. Lytova, E. Lorin, and A. D. Bandrauk, *Propagation of intense and short circularly polarized pulses in a molecular gas: From multiphoton ionization to nonlinear macroscopic effects*, Phys. Rev. A, 94, 013421.

[33] R. McOwen, *Partial Differential Equations : methods and applications*, Pearson Education, Inc, Upper Saddle River, New Jersey 07458, 2003.

[34] A. McPherson, G. Gibson, H. Jara, U. Johann, T. S. Luk, I. A. McIntyre, K. Boyer, and C. K. Rhodes, *Studies of multiphoton production of vacuum-ultraviolet radiation in the rare gases*, J. Opt. Soc. of Am. B, 4 (1987), pp. 595–601.

[35] T. Morishita, A.-T. Le, Z. Chen, and C. D. Lin, *Accurate retrieval of structural information from laser-induced photoelectron and high-order harmonic spectra by few-cycle laser pulses*, Phys. Rev. Lett., 100 (2008), 013903.

[36] A. Newell, *Short pulse evolution equation*, in Laser Filamentation. Mathematical Methods and Models, A.Bandrauk, E.Lorin and J.Moloney, eds., (2016), pp. 1–17.

[37] A. Newell and J. Moloney, *Nonlinear Optics*, Advanced Topics in the Interdisciplinary Mathematical Sciences, Addison-Wesle Publishing Company, 1992.

[38] P. Panagiotopoulos, P. Whalen, M. Kolesik, and J. Moloney, *Numerical simulation of ultra-short laser pulses*, in Laser Filamentation. Mathematical Methods and Models, A.Bandrauk, E.Lorin and J.Moloney, eds., (2016), pp. 185–213.

[39] P. Polynkin, M. Kolesik, E. Wright, and J. Moloney, *Experimental tests of the new paradigm for laser filamentation in gases*, Phys. Rev. Lett., 106 (2011), 153902.

[40] M. Richter, S. Patchkovskii, F. Morales, O. Smirnova, and M. Ivanov, *The role of the Kramers-Henneberger atom in the higher-order Kerr effect*, New J. Phys., 15 (2013), 083012.

[41] K. Schafer, B. Yang, L. Dimauro, and K. Kulander, *Above threshold ionization beyond the high harmonic cutoff*, Phys. Rev. Lett., 70 (1993), pp. 1599–1602.

[42] S. Skupin and L. Bergé, *Self-guiding of femtosecond light pulses in condensed media: Plasma generation versus chromatic dispersion*, Physica D, 220 (2006), pp. 14–30.

[43] A. Spott, A. Jaro-Becker, and A. Becker, *Ab initio and perturbative calculations of the electric susceptibility of atomic hydrogen*, Phys. Rev. A, 90 (2014), 013426.

[44] G. Strang, *On the construction and comparison of difference schemes*, SIAM J. Numer. Anal., 5 (1968), pp. 506–517.

[45] V. Strelkov, *High-order optical processes: towards nonperturbative nonlinear optics*, preprint, arXiv:1504.07871 [physics.atom-ph].

[46] J. Strikwerda, *Finite Difference Schemes and Partial Differential Equations.*, Society for Industrial and Applied Mathematics (SIAM), Philadelphia, PA, 2nd ed., 2004.

[47] M. Taylor, *Partial Differential Equations I. Basic Theory.*, Springer, 2nd ed., 2011.

[48] A. Vinçotte and L. Bergé, *Atmospheric propagation of gradient-shaped and spinning femtosecond light pulses*, Phys. D, 223 (2006), pp. 163–173.

[49] H.-M. Yin, *Existence and regularity of a weak solution to Maxwell's equations with a thermal effect*, Math. Methods Appl. Sci., 29 (2006), pp. 1199–1213.

[50] K.-J. Yuan, S. Chelkowski, and A. Bandrauk, *Molecular photoelectron angular distribution rotation in multi-photon resonant ionization of H_2^+ by circularly polarized ultraviolet laser pulses*, J. Chem. Phys., 142 (2015), 144303.